Topic	The new IASPEI standards for determining magnitudes from digital data and their relation to classical magnitudes
Authors	**Peter Bormann** (formerly GFZ German Research Centre for Geosciences, Dept. 2, D-14473 Potsdam, Germany); E-mail: pb65@gmx.net **James W. Dewey**, U. S. Geological Survey, MS 966, Denver, CO 80225-0046; Phone: 303 273 8419, E-mail: jdewey@usgs.gov
Version	March 2012; **DOI: 10.2312/GFZ.NMSOP-2_IS_3.3**

Note: Figure and Table numbers followed in this text by ??? relate to the NMSOP editions 2002 (printed) and 2009 (website). They will be changed when the revised Chapters 3 and 11 of NMSOP-2 become available.

1 Why there is a need for measurement standards of magnitudes

In October 2005, the Commission on Seismic Observation and Interpretation of the International Association of Seismology and Physics of the Earth´s Interior (IASPEI) adopted the summary recommendations made by the IASPEI Working Group on Magnitudes on new measurement standards for widely used local, regional and teleseismic magnitude scales (IASPEI, 2005). These recommendations have recently been refined and detailed (IASPEI, 2013) and a final scientific report, to be published in a reputable international journal, is currently under preparation.

The Working Group has been established by the IASPEI General Assembly 2001 in Hanoi, following a request of the Governing Council of the International Seismological Center (ISC). The latter was concerned about significant discrepancies between short-period body-wave magnitudes mb determined by the US Geological Survey´s National Earthquake Information Center (USGS/NEIC) and the Prototype International Data Centre (PIDC), predecessor to the International Data Centre (IDC) of the Comprehensive Test-Ban Treaty Organization (CTBTO) at Vienna. Since then, significant causes of these discrepancies have been identified as coming from differences in the applied short-period filter response, in the length of the measurement time window (Granville et al., 2002 and 2005; Bormann et al., 2007 and 2009) and in the different calibration functions used (Gutenberg and Richter, 1956a, and Veith and Clawson, 1972, respectively; in the following abbreviated by G-R and V-C) for correcting the effects of epicentral distance and source depth on the measured amplitudes (Murphy and Barker, 2003; Granville et al., 2005). The average discrepancy between mb(NEIC) and mb(IDC) was found to be approximately +0.4 magnitude units (m.u.) (Granville et al., 2002). This difference, however, strongly increases with magnitude and is larger than 1 m.u. for really great earthquakes (e.g., 1.3 m.u. for the 2004 Mw9.3 Sumatra-Andaman earthquake; see Bormann et al., 2007). Further, the differences are smaller for shallow earthquakes than for deep earthquakes, because for source depths h > 300 km the V-C corrections are on average 0.4 m.u. (up to 0.6 m.u. for the deepest earthquakes) smaller than the G-R corrections. Despite these systematic discrepancies, the USGS/NEIC and the IDC publish their body-wave magnitude with the same symbol mb.

Similarly, the symbol Ms is commonly used both for surface-wave magnitudes based on amplitude measurements around 20 sec period and those measured in a much wider period range. For both Ms measured near 20s and Ms measured over broader period ranges, multiple attenuation functions have been proposed. These may produce magnitudes that differ systematically (sometimes up to about 0.6 m.u.), especially for smaller earthquakes recorded only at distances < 30° (Bormann et al., 2009).

Publishing magnitudes derived by different measurement procedures with identical magnitude symbols may not only confuse and mislead users of such data, it also jeopardizes the authenticity, compatibility and long-term continuity of magnitude data and thus their use in earthquake statistics and related applications. For example, when merging mb(NEIC) and mb(IDC) data at the ISC for calculating event averages and standard deviations, systematic differences and increased data scatter may significantly bias such estimates for magnitudes larger than 5. Therefore, IASPEI realized a general need to identify such discrepancies in measurement practices of widely determined different types of magnitudes, to analyze, quantify and understand the reasons for such discrepancies and to propose international standards for making such measurements.

2 Aim of the proposed magnitude standards

IASPEI recommended that measurement standards for magnitudes should, as far as possible:

- agree with magnitudes of the same type that have been measured for decades from analog seismograms according to original definitions;
- promote the best possible use of the advantages of digital data and processing;
- minimize bulletin magnitude biases that result from procedure-dependent single-station or network magnitude biases;
- increase the number of seismological stations and networks with well-defined procedures;
- increase essentially the accuracy, representativeness, homogeneity and long-term global compatibility of magnitude data and their usefulness for seismic hazard assessment and research.

3 Summary recommendations on determining earthquake magnitudes from digital data

The Working Group on Magnitudes (for short, *Magnitude WG)* of the IASPEI Commission on Seismological Observation and Interpretation was established to recommend standard procedures for making measurements from digital data to be used in calculating several widely used types of earthquake magnitude. The recommended procedures from the *Magnitude WG* have been approved by the IASPEI Commission on Seismological Observations and Interpretations. We henceforth refer to the proposed procedures as the IASPEI standard procedures for magnitude determination. The *Magnitude WG* is planning to publish an article, in the open literature, that explains the rationale for the IASPEI standard procedures. Current members of the *Magnitude WG* are, in alphabetical order: P. Bormann (co-chair), J. M. Dewey (co-chair), I. Gabsatarova, S. Gregersen, A. Gusev, W. Kim, R. Liu, H. Patton, B. Presgrave, J. Saul, R. A. Uhrhammer, S. Wendt.

The IASPEI standard procedures address the measurement of amplitudes and periods from digital data for use in calculating the generic magnitude types *ML*, *Ms*, *mb*, *mB*, and *mb_Lg*. For *Ms*, standard procedures are proposed for two different traditions -- *Ms* measured from waves with periods near 20s [here denoted *Ms_20*] and *Ms* measured from waves in a much broader period-range [here denoted *Ms_BB*]. For the generic intermediate-period/broadband body-wave magnitude *mB*, we propose a procedure based on the maximum amplitude of the *P*-wave measured on a velocity-proportional trace: we denote the resulting magnitude *mB_BB*. The IASPEI standard procedures also specify a standard equation for *Mw* from among several slightly different equations. Abbreviated descriptions of the procedures are described below. More detailed descriptions, and discussion of acceptable alternatives to specific steps in the application of individual procedures, will be discussed in the planned journal article and in the last section of this Information Sheet.

Some of the IASPEI standard procedures require the use of broadband (BB) records that are proportional to ground motion velocity at least within the period range that has been recommended for the measurement of the respective magnitudes. Other procedures require

filtering BB records so that they replicate the response of classical standard seismographs, such as the Wood-Anderson (WA) seismograph or the short-period (SP) and long-period (LP) seismographs that were used in the World-Wide Standardized Seismograph Network (WWSSN) (next section).

3.1 Poles and zeroes for Wood-Anderson, WWSSN-SP, and WWSSN-LP seismographs

Poles and zeroes corresponding to the displacement transfer functions for representative "average" classical analog standard seismographs WWSSN-SP, WWSSN-LP and Wood Anderson with their equivalent eigenperiod and damping of the seismometer and galvanometer and coupling factor σ^2 (where applicable) are given in Table 1 (courtesy of Charles R. Hutt, U. S. Geological Survey, who also provided much of the immediately following documentation). Note that the number of zeroes determines the slope of the response at the low-frequency end and that this slope changes towards higher frequencies at the frequencies determined by the poles. At the frequency of a conjugate complex pole the slope is reduced by two orders, while at a single pole with real part only, the slope is reduced by one order only. The left number in brackets is the value of the real part; the right number that of the imaginary part. The normalized amplitude responses corresponding to the poles and zeroes of Table 1 are shown in Figure 1.

At magnifications of 50,000 and higher, transfer functions for the WWSSN short-period seismograph differed somewhat for different magnification settings, due to galvanometer-seismometer reaction. The response shown in Table 1 and recommended for use with *mb* is appropriate to a "100,000 magnification" short-period WWSSN seismograph.

Transfer functions for the WWSSN long-period seismograph also differed somewhat for different magnification settings, due to galvanometer-seismometer reaction. The response shown in Table 1 is appropriate to a "1500 magnification" long-period vertical WWSSN seismograph. The transfer functions of the WWSSN-LP horizontal seismograph also differed from that of the WWSSN-LP vertical seismograph. One should note that the coupling which exists in electromagnetic seismographs with galvanometric recording between the seismometer and galvanometer has been taken into account in the listed poles in such a way as to make the coupling factor effectively zero. Accordingly, the resulting free periods and damping values given for the equivalent seismometer (T_s and h_s) and galvanometer (T_g and h_g) in Table 1 are somewhat different from the nominal values of the uncoupled system components of classical seismographs and the respective coupling factors are reported as zero. The nominal free periods of the uncoupled components are T_s = 1.00 s and T_g = 0.75 s for WWSSN-SP and T_s = 15.0 s and T_g = 100.0 s for WWSSN-LP.

The frequency response of the Wood-Anderson seismograph (Table 1) is based on the paper of Uhrhammer and Collins (1990).

Table 1 Zeroes and poles corresponding to the displacement transfer function of the WWSSN-SP seismograph, WWSSN-LP seismograph, and the Wood-Anderson (WA) seismograph. Zeroes and poles are represented in angular frequency (radians per second). T_S = seismometer free period; h_s = seismometer damping constant; T_g = galvanometer free period; h_g = galvanometer damping constant; σ^2 = coupling factor. In this representation, free periods and damping constants have been adjusted slightly so that response can be correctly modeled with $\sigma^2 = 0$. The displacement-response functions implied by the poles and zeroes are commonly normalized with respect to the following frequencies (f_n) using the associated normalization factors ($A_{o)}$ as follows: WWSSN-SP, $f_n = 1$ Hz, $A_o = 532.14$; WWSSN-LP, $f_n = 0.04$ Hz, $A_o = 0.97866$; WA, $f_n = 4$ Hz, $A_o = 1.0028$.

Seismograph	Zeros	Poles	T_s/s	h_s	T_g/s	h_g
WWSSN-SP	(0.0, 0.0) (0.0, 0.0) (0.0, 0.0)	(-3.72500, -6.22000) (=p_1) (-3.72500, 6.22000) (=p_2) (-5.61200, 0.00000) (=p_3) (-13.2400, 0.00000) (=p_4) (-21.0800, 0.00000) (=p_5)	0.867	0.5138	0.729	1.0935
WWSSN-LP	(0.0, 0.0) (0.0, 0.0) (0.0, 0.0)	(-0.40180, 0.08559) (-0.40180, 0.08559) (-0.04841, 0.00000) (-0.08816, 0.00000)	15.29	0.978	96.18	1.045
WA	(0.0, 0.0) (0.0, 0.0)	(-5.49779, -5.60886) (-5.49779, 5.60886)	0.8	0.7		

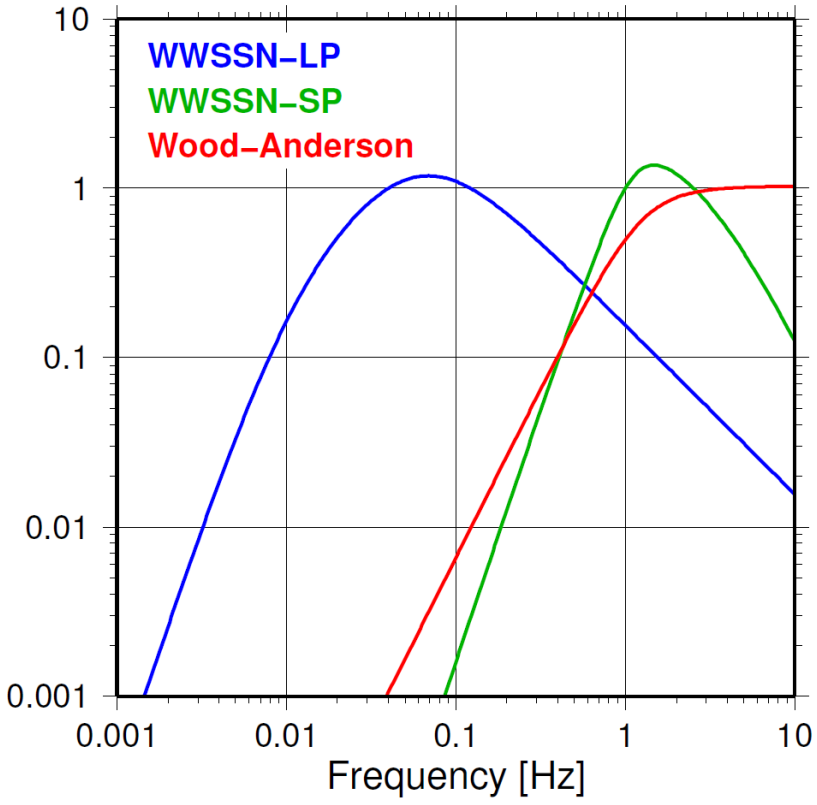

Figure 1 Displacement amplitude-frequency responses of the classical seismographs: WWSSN-SP, WWSSN-LP and Wood-Anderson (WA), normalized to the frequencies (f_n) in the caption of Table 1.

3.2 IASPEI standard procedures for widely used magnitude types

The amplitudes used in the magnitude formulas below are in most circumstances to be measured as one-half the maximum deflection of the seismogram trace, peak-to-adjacent-trough or trough-to-adjacent-peak, where peak and trough are separated by one crossing of the zero-line: the measurement is sometimes described as "one-half peak-to-peak amplitude." None of the magnitude formulas presented in this article are intended to be used with the full peak-to-trough deflection as the amplitude. The periods are to be measured as twice the time-intervals separating the peak and adjacent-trough from which the amplitudes are measured. The amplitude-phase arrival-times are to be measured as the time of the zero-crossing between the peak and adjacent-trough from which the amplitudes are measured. The issue of amplitude and period measuring procedures, and circumstances under which alternative procedures are acceptable or preferable, is discussed further in Section 5.

Modern digital seismogram analysis programs commonly measure amplitudes in units of nm (for displacement) or nm/s (for velocity), respectively, and not, as assumed by the classical magnitude formulas, in μm. The commonly known classical calibration relationships have been modified to be consistent with displacements measured in nm.

***ML** – local magnitude consistent with the magnitude of Richter (1935)*

For crustal earthquakes in regions with attenuative properties **similar** to those of Southern California, the proposed standard equation is

$$ML = \log_{10}(A) + 1.11 \log_{10}R + 0.00189*R - 2.09, \quad (1)$$

where:

A = maximum **trace** amplitude in **nm** that is measured on output from a **horizontal-component** instrument that is filtered so that the response of the seismograph/filter system replicates that of a **Wood-Anderson standard seismograph** but with a static magnification of 1 (see Table 1 and Figure 1);

R = **hypocentral distance in km**, typically less than 1000 km.

Equation (1) is an expansion of that of Hutton and Boore (1987). The constant term in equation (1), -2.09, is based on an experimentally determined static magnification of the Wood-Anderson of 2080, rather than the theoretical magnification of 2800 that was specified by the seismograph´s manufacturer. The formulation of equation (1) reflects the intent of the *Magnitude WG* that reported *ML* amplitude data not be affected by uncertainty in the static magnification of the Wood-Anderson seismograph.

For seismographic stations containing two horizontal components, amplitudes are measured independently from each horizontal component, and each amplitude is treated as a single datum. There is no effort to measure the two observations at the same time, and there is no attempt to compute a vector average.

For crustal earthquakes in regions with attenuative properties that are **different** than those of coastal California, and for measuring magnitudes with vertical-component seismographs, the standard equation is of the form:

$$ML = \log_{10}(A) + C(R) + D, \quad (2)$$

where A and R are as defined in equation (1), except that A may be measured from a **vertical-component** instrument, and where $C(R)$ and D have been **calibrated** to adjust for the different regional attenuation and to adjust for any systematic differences between amplitudes measured on horizontal seismographs and those measured on vertical seismographs.

Ms_20 *– teleseismic surface-wave magnitudes at period of ~20* s

$$Ms\_20 = \log_{10}(A/T) + 1.66\log_{10}\Delta + 0.3, \quad (3)$$

where:

A = **vertical-component** ground displacement in **nm** measured from the maximum trace-amplitude of a surface-wave phase having a period between **18 s and 22 s** on a waveform that has been filtered so that the frequency response of the seismograph/filter system replicates that of a World-Wide Standardized Seismograph Network (WWSSN) **long-period seismograph** (see Table 1), with A being determined by dividing the maximum trace amplitude by the magnification of the simulated WWSSN-LP response at period T;

T = period in seconds ($18 \text{ s} \le T \le 22$ s);

Δ = **epicentral** distance in degrees**, $20° \le \Delta \le 160°$**;

Equation (3) is formally equivalent to the *Ms* equation proposed by Vaněk et al. (1962) but is here applied to vertical motion measurements in a narrow range of periods.

Some agencies compute *Ms_20* only for shallow-focus earthquakes (typically those whose confidence-intervals on focal-depth would allow them to be shallower than 50 or 60 km). *Ms_20* would be expected to significantly under-represent the energy of intermediate- and deep-focus earthquakes, due to their less effective generation of surface waves, unless an adjustment is made to account for their large focal-depths, e.g., according to Herak et al. (2001).

Ms_BB *– surface-wave magnitudes from broad-band instruments*

$$Ms\_BB = \log_{10}(V_{max}/2\pi) + 1.66\log_{10}\Delta + 0.3, \quad (4)$$

where:

V_{max} = ground **velocity *in* nm/s** associated with the maximum trace-amplitude in the surface-wave train, as recorded on a **vertical-component** seismogram that is **proportional to velocity**, where the period of the surface-wave, *T*, should satisfy the condition **3 s < *T* < 60 s**, and where *T* should be preserved together with V_{max} in bulletin data-bases;

Δ = **epicentral** distance in degrees, **2° ≤ Δ ≤ 160°**

As with *Ms_20*, some agencies compute *Ms_BB* only for shallow-focus earthquakes.

Equation (4) is based on the *Ms* equation proposed by Vaněk et al. (1962), but is here applied to vertical motion measurements and is used with the $\log_{10}(V_{max}/2\pi)$ term replacing the $\log_{10}(A/T)_{max}$ term of the original.

---

mb *– short-period body-wave magnitude*

$$mb = \log_{10}(A/T) + Q(\Delta, h) - 3.0, \quad (5)$$

where:

A = P-wave ground amplitude in **nm** calculated from the maximum trace-amplitude in the **entire P-phase train** (time spanned by P, pP, sP, and possibly PcP and their codas, and ending preferably before PP);

T = period in seconds, ***T* < 3 s**; of the maximum P-wave trace amplitude.

$Q(\Delta, h)$ = attenuation function for **PZ** (P-waves recorded on vertical component seismographs) established by **Gutenberg and Richter (1956a)** in the tabulated or algorithmic form as used by the U.S. Geological Survey/National Earthquake Information Center (USGS/NEIC) (**Table 2**);

Δ = **epicentral** distance in degrees, **20° ≤ Δ ≤ 100°**;

h = focal depth in **km**;

and where both *T* and the maximum trace amplitude are measured on output from a **vertical-component** instrument that is filtered so that the frequency response of the seismograph/filter system replicates that of a WWSSN **short-period** seismograph (**Table 1**), with *A* being determined by dividing the maximum trace amplitude by the magnification of the simulated WWSSN-SP response at period *T*.

---

mB_BB *– broadband body-wave magnitude*

$$mB\_BB = \log_{10}(V_{max}/2\pi) + Q(\Delta, h) - 3.0, \quad (6)$$

where:

V_{max} = ground **velocity *in* nm/s** associated with the maximum trace-amplitude in **the entire P-phase train** (time spanned by P, pP, sP, and possibly PcP and their codas, but ending ***preferably*** before PP (*Note*: *see discussion in the final section*), as recorded on a vertical-component seismogram that is **proportional to velocity,** where the period of the measured phase, *T*, should satisfy the condition **0.2 s < *T* < 30 s**, and where *T* should be preserved together with V_{max} in bulletin data-bases;

$Q(\Delta, h)$ = attenuation function for PZ established by Gutenberg and Richter (1956a), (**Table 2**);

Δ = epicentral distance in degrees, **$20° \leq \Delta \leq 100°$**;

h = focal depth in **km**.

Equation (6) differs from the equation for m_B of Gutenberg and Richter (1956a) by virtue of the $\log_{10}(V_{max}/2\pi)$ term, which replaces the classical $\log_{10}(A/T)_{max}$ term.

Table 2 Attenuation (Q) function to be used with *mb* (equation 5) and *mB_BB* (equation 6). This version of $Q(\Delta, \textit{focal-depth})$ was digitized in the 1960's from Figure 5 of Gutenberg and Richter (1956a) and is used at the USGS/NEIC. This is a comma-delimited file, intended to be copied into applications, with the first two rows being header rows. The first column is epicentral distance D (= Δ) in degrees, and the following columns give Q for distance D and depths 0, 25, …700 km. For D and focal-depth lying between tabulated values, *Q* is obtained by linear interpolation from the four neighboring tabulated values.

```
D, Focal Depth (km),,,,,,,,,,,,,,,,
  ,0.0, 25, 50, 75,100,150,200,250,300,350,400,450,500,550,600,650,700
20,6.1,6.1,6.1,6.1,6.1,6.2,6.3,6.3,6.1,6.1,6.2,6.3,6.4,6.4,6.4,6.2,6.0
21,6.1,6.2,6.1,6.1,6.1,6.2,6.3,6.3,6.1,6.1,6.2,6.3,6.4,6.4,6.4,6.2,6.0
22,6.2,6.2,6.2,6.2,6.1,6.2,6.3,6.3,6.1,6.1,6.2,6.3,6.4,6.4,6.4,6.3,6.1
23,6.3,6.3,6.2,6.2,6.1,6.2,6.4,6.3,6.2,6.1,6.2,6.3,6.4,6.4,6.4,6.3,6.1
24,6.4,6.3,6.3,6.2,6.2,6.3,6.4,6.3,6.2,6.1,6.2,6.3,6.3,6.4,6.4,6.4,6.1
25,6.5,6.4,6.3,6.2,6.2,6.3,6.4,6.3,6.2,6.1,6.2,6.3,6.3,6.4,6.4,6.4,6.2
26,6.5,6.4,6.3,6.3,6.3,6.4,6.5,6.4,6.2,6.1,6.2,6.2,6.3,6.4,6.4,6.4,6.2
27,6.5,6.4,6.4,6.3,6.3,6.4,6.5,6.4,6.2,6.1,6.2,6.2,6.3,6.4,6.4,6.4,6.3
28,6.6,6.5,6.4,6.4,6.4,6.5,6.5,6.4,6.3,6.1,6.1,6.2,6.3,6.4,6.4,6.4,6.3
29,6.6,6.5,6.4,6.4,6.4,6.5,6.5,6.4,6.3,6.1,6.1,6.2,6.3,6.4,6.4,6.4,6.3
30,6.6,6.6,6.5,6.5,6.5,6.5,6.5,6.4,6.3,6.1,6.1,6.2,6.3,6.4,6.4,6.4,6.3
31,6.7,6.6,6.5,6.5,6.5,6.5,6.5,6.4,6.3,6.1,6.1,6.2,6.3,6.4,6.4,6.4,6.3
32,6.7,6.7,6.6,6.6,6.5,6.6,6.4,6.4,6.3,6.1,6.1,6.2,6.3,6.4,6.4,6.4,6.4
33,6.7,6.7,6.6,6.6,6.6,6.5,6.4,6.4,6.3,6.1,6.1,6.2,6.3,6.4,6.4,6.4,6.4
34,6.7,6.7,6.7,6.7,6.6,6.5,6.4,6.4,6.3,6.1,6.1,6.2,6.3,6.4,6.4,6.4,6.3
35,6.6,6.7,6.7,6.7,6.7,6.5,6.4,6.3,6.3,6.1,6.1,6.2,6.3,6.4,6.4,6.3,6.3
36,6.6,6.7,6.7,6.7,6.7,6.5,6.4,6.3,6.3,6.1,6.1,6.2,6.3,6.4,6.4,6.3,6.3
37,6.5,6.6,6.7,6.7,6.7,6.5,6.4,6.3,6.2,6.1,6.1,6.2,6.3,6.4,6.4,6.3,6.3
38,6.5,6.6,6.7,6.7,6.7,6.5,6.4,6.3,6.2,6.1,6.1,6.2,6.3,6.4,6.3,6.3,6.3
39,6.4,6.5,6.6,6.7,6.6,6.5,6.4,6.3,6.1,6.0,6.1,6.2,6.3,6.4,6.3,6.3,6.3
40,6.4,6.5,6.6,6.7,6.6,6.5,6.3,6.2,6.1,6.0,6.1,6.2,6.3,6.4,6.3,6.2,6.3
41,6.5,6.5,6.5,6.6,6.6,6.4,6.3,6.2,6.0,6.0,6.1,6.2,6.3,6.3,6.3,6.2,6.3
42,6.5,6.5,6.5,6.6,6.6,6.4,6.3,6.2,6.0,6.0,6.1,6.2,6.3,6.3,6.3,6.2,6.3
43,6.5,6.5,6.5,6.6,6.6,6.4,6.3,6.1,6.0,6.0,6.1,6.2,6.3,6.3,6.3,6.2,6.3
44,6.6,6.6,6.5,6.6,6.6,6.4,6.3,6.1,6.1,6.0,6.1,6.2,6.3,6.3,6.3,6.2,6.2
45,6.7,6.7,6.6,6.6,6.6,6.4,6.2,6.1,6.1,6.0,6.1,6.2,6.3,6.3,6.3,6.2,6.2
```

```
 D, Focal Depth (km)(continuation),,,,,,,,,,,,,,,
   ,0.0, 25, 50, 75,100,150,200,250,300,350,400,450,500,550,600,650,700
 46,6.8,6.7,6.7,6.7,6.6,6.4,6.2,6.1,6.1,6.0,6.1,6.2,6.3,6.3,6.3,6.2,6.2
 47,6.9,6.8,6.7,6.7,6.6,6.4,6.2,6.1,6.1,6.0,6.1,6.2,6.3,6.3,6.3,6.2,6.2
 48,6.9,6.8,6.8,6.7,6.6,6.5,6.2,6.1,6.1,6.0,6.1,6.2,6.2,6.3,6.3,6.2,6.2
 49,6.8,6.8,6.8,6.8,6.7,6.5,6.2,6.2,6.1,6.1,6.1,6.2,6.2,6.3,6.3,6.2,6.2
 50,6.7,6.8,6.8,6.8,6.8,6.5,6.3,6.2,6.1,6.1,6.1,6.1,6.2,6.3,6.3,6.1,6.1
 51,6.7,6.7,6.8,6.8,6.8,6.5,6.3,6.2,6.2,6.1,6.1,6.1,6.2,6.2,6.2,6.1,6.1
 52,6.7,6.7,6.8,6.8,6.8,6.5,6.4,6.2,6.2,6.1,6.1,6.1,6.1,6.2,6.2,6.1,6.1
 53,6.7,6.7,6.8,6.8,6.8,6.6,6.4,6.2,6.2,6.1,6.1,6.1,6.1,6.1,6.2,6.1,6.1
 54,6.8,6.8,6.8,6.8,6.8,6.6,6.4,6.3,6.2,6.1,6.1,6.1,6.1,6.1,6.1,6.1,6.0
 55,6.8,6.8,6.8,6.8,6.8,6.6,6.5,6.3,6.2,6.2,6.1,6.1,6.1,6.1,6.1,6.0,6.0
 56,6.8,6.8,6.8,6.8,6.8,6.7,6.5,6.3,6.2,6.2,6.1,6.1,6.1,6.1,6.1,6.0,6.0
 57,6.8,6.8,6.8,6.9,6.8,6.7,6.5,6.4,6.2,6.2,6.2,6.2,6.1,6.1,6.0,6.0,6.0
 58,6.8,6.8,6.9,6.9,6.8,6.7,6.5,6.4,6.3,6.2,6.2,6.2,6.1,6.1,6.0,6.0,6.0
 59,6.9,6.9,6.9,6.9,6.9,6.7,6.5,6.4,6.3,6.2,6.2,6.2,6.2,6.1,6.0,6.0,6.0
 60,6.9,6.9,6.9,6.9,6.9,6.7,6.5,6.4,6.3,6.3,6.2,6.2,6.2,6.1,6.0,6.0,6.0
 61,6.9,6.9,6.9,6.9,6.8,6.7,6.5,6.4,6.3,6.3,6.3,6.3,6.2,6.2,6.1,6.0,6.0
 62,7.0,6.9,6.9,6.9,6.8,6.7,6.6,6.4,6.4,6.3,6.3,6.3,6.3,6.2,6.1,6.1,6.0
 63,7.0,6.9,6.9,6.8,6.7,6.7,6.6,6.5,6.4,6.4,6.4,6.3,6.3,6.2,6.2,6.1,6.0
 64,7.0,6.9,6.8,6.7,6.7,6.7,6.6,6.5,6.5,6.4,6.4,6.4,6.4,6.3,6.2,6.1,6.1
 65,7.0,6.9,6.8,6.7,6.7,6.7,6.6,6.5,6.5,6.5,6.4,6.4,6.4,6.3,6.2,6.1,6.1
 66,7.0,6.9,6.8,6.7,6.7,6.7,6.5,6.5,6.5,6.5,6.5,6.4,6.4,6.3,6.2,6.2,6.1
 67,7.0,6.9,6.8,6.7,6.7,6.6,6.5,6.5,6.5,6.5,6.5,6.4,6.4,6.3,6.3,6.2,6.1
 68,7.0,6.9,6.8,6.7,6.7,6.6,6.5,6.5,6.5,6.5,6.5,6.4,6.4,6.3,6.3,6.2,6.2
 69,7.0,6.9,6.7,6.7,6.6,6.6,6.5,6.5,6.5,6.5,6.4,6.4,6.4,6.3,6.3,6.2,6.2
 70,6.9,6.9,6.7,6.7,6.6,6.6,6.5,6.5,6.5,6.5,6.4,6.4,6.3,6.3,6.3,6.2,6.2
 71,6.9,6.9,6.7,6.7,6.6,6.6,6.5,6.5,6.5,6.5,6.4,6.4,6.3,6.3,6.3,6.3,6.2
 72,6.9,6.8,6.7,6.7,6.6,6.5,6.5,6.5,6.5,6.5,6.4,6.4,6.3,6.3,6.3,6.3,6.2
 73,6.9,6.8,6.7,6.7,6.6,6.5,6.5,6.5,6.5,6.5,6.4,6.4,6.3,6.3,6.3,6.3,6.3
 74,6.8,6.8,6.7,6.7,6.6,6.5,6.5,6.5,6.5,6.5,6.4,6.4,6.3,6.3,6.3,6.3,6.3
 75,6.8,6.8,6.7,6.7,6.6,6.5,6.5,6.5,6.5,6.5,6.5,6.4,6.3,6.2,6.3,6.3,6.3
 76,6.9,6.8,6.7,6.7,6.6,6.5,6.5,6.5,6.5,6.5,6.5,6.4,6.3,6.2,6.3,6.3,6.3
 77,6.9,6.8,6.8,6.7,6.6,6.5,6.5,6.5,6.5,6.6,6.5,6.4,6.2,6.2,6.2,6.3,6.3
 78,6.9,6.8,6.8,6.7,6.6,6.5,6.5,6.5,6.5,6.6,6.5,6.4,6.2,6.2,6.2,6.3,6.3
 79,6.8,6.8,6.7,6.7,6.6,6.5,6.5,6.5,6.6,6.6,6.5,6.4,6.2,6.2,6.2,6.3,6.3
 80,6.7,6.8,6.7,6.7,6.6,6.5,6.5,6.5,6.6,6.6,6.5,6.4,6.2,6.2,6.2,6.3,6.3
 81,6.8,6.8,6.7,6.7,6.6,6.5,6.5,6.5,6.6,6.6,6.5,6.4,6.3,6.3,6.3,6.3,6.3
 82,6.9,6.8,6.8,6.7,6.6,6.5,6.5,6.5,6.6,6.6,6.5,6.4,6.3,6.3,6.3,6.3,6.3
 83,7.0,6.9,6.8,6.7,6.7,6.6,6.5,6.5,6.6,6.6,6.5,6.5,6.3,6.3,6.3,6.4,6.3
 84,7.0,7.0,6.8,6.8,6.7,6.6,6.5,6.6,6.6,6.6,6.5,6.5,6.4,6.4,6.4,6.4,6.3
 85,7.0,7.0,6.9,6.8,6.7,6.6,6.5,6.6,6.6,6.6,6.6,6.5,6.4,6.4,6.4,6.4,6.4
 86,6.9,7.0,7.0,6.8,6.8,6.6,6.6,6.6,6.6,6.6,6.7,6.6,6.5,6.5,6.5,6.5,6.5,6.4
 87,7.0,7.0,7.0,6.9,6.8,6.7,6.6,6.6,6.7,6.7,6.6,6.5,6.5,6.5,6.5,6.5,6.4
 88,7.1,7.1,7.0,6.9,6.8,6.8,6.6,6.6,6.7,6.7,6.6,6.6,6.6,6.6,6.6,6.5,6.4
 89,7.0,7.1,7.1,7.0,6.9,6.8,6.7,6.7,6.7,6.7,6.6,6.6,6.6,6.7,6.7,6.6,6.5
 90,7.0,7.0,7.1,7.0,6.9,6.8,6.7,6.7,6.7,6.7,6.6,6.7,6.7,6.7,6.7,6.7,6.5
 91,7.1,7.1,7.2,7.1,7.0,6.9,6.8,6.7,6.7,6.7,6.7,6.7,6.7,6.8,6.8,6.7,6.6
 92,7.1,7.2,7.2,7.2,7.1,6.9,6.8,6.8,6.7,6.8,6.7,6.8,6.8,6.8,6.8,6.8,6.7
 93,7.2,7.2,7.2,7.2,7.1,7.0,6.9,6.8,6.8,6.8,6.8,6.8,6.8,6.9,6.8,6.9,6.7
 94,7.1,7.2,7.2,7.2,7.2,7.0,6.9,6.9,6.9,6.9,6.9,6.9,6.9,7.0,6.9,6.8
 95,7.2,7.2,7.2,7.2,7.2,7.1,7.0,7.0,6.9,6.9,6.9,6.9,6.9,7.0,7.0,7.0,6.9
 96,7.3,7.2,7.3,7.3,7.3,7.2,7.1,7.0,7.0,7.0,6.9,7.0,7.0,7.0,7.0,7.0,6.9
 97,7.4,7.3,7.3,7.3,7.3,7.2,7.1,7.1,7.0,7.0,7.0,7.0,7.1,7.1,7.1,7.0,7.0
 98,7.5,7.3,7.3,7.3,7.3,7.3,7.2,7.1,7.1,7.1,7.1,7.1,7.1,7.1,7.1,7.1,7.0
 99,7.5,7.3,7.3,7.3,7.4,7.3,7.2,7.2,7.2,7.1,7.1,7.2,7.2,7.2,7.2,7.1,7.0
100,7.3,7.3,7.3,7.4,7.4,7.3,7.2,7.2,7.2,7.2,7.2,7.2,7.2,7.2,7.2,7.2,7.1

-----------------------------------------------------------------------
```

mb_Lg *– regional magnitude based on the amplitude of Lg measured in a narrow period range around 1 s*

$$mb\_Lg = \log_{10}(A) + 0.833\log_{10}[r] + 0.4343\gamma(r - 10) - 0.87 \quad (7)$$

where:

A = "sustained ground-motion amplitude" in **nm**, defined as the third largest amplitude in the time window corresponding to group velocities of 3.6 to 3.2 *km/s*, in the period (T) range 0.7 s to 1.3 s;

r = **epicentral distance** in **km**

γ = coefficient of attenuation in km^{-1}. γ is related to the quality factor Q through the equation $\gamma = \pi/(Q \cdot U \cdot T)$, where U is group velocity and T is the wave period of the L_g wave. γ is a strong function of crustal structure and should be determined specifically for the region in which the *mb_Lg* is to be used.

A and *T* are measured on output from a **vertical-component** instrument that is filtered so that the frequency response of the seismograph/filter system replicates that of a WWSSN **short-period** seismograph. Arrival times with respect to the origin of the seismic disturbance are used, along with epicentral distance, to compute group velocity *U*.

Mw *– moment magnitude*

$$Mw = (\log_{10}M_0 - 9.1)/1.5,$$

where M_0 = scalar moment in **N·m**, determined from waveform modeling or from the long-period asymptote of spectra.

or its CGS equivalent (M_0 in **dyne·cm**),

$$Mw = (\log_{10}M_0 - 16.1)/1.5.$$

The order of operations in the right-hand sides of equations for Mw, subtraction prior to multiplication by 2/3, avoids an ambiguity that arises if multiplication is performed prior to subtraction, which in a certain percentage of cases leads to Mw being different according to whether the moment is expressed in CGS or SI units (Utsu, 2002). In this context it may be worth mentioning, that P. Bormann and G. Choy have agreed on the same way of standardized writing of the energy magnitude relationship $Me = (\log E_S - 4.4)/1.5$ instead of the expanded and rounded-off version $Me = (2/3)\log E_S - 2.9$.

3.3 Magnitude nomenclature

The *"ML, Ms_20, Ms_BB, mb, mB_BB, Mw, mb_Lg"* nomenclature used in this section of IS_3.3 is defined to facilitate data transmission in the IASPEI Seismic Format (ISF) (International Seismological Centre, http://www.isc.ac.uk/standards/isf, last accessed March

2012). In the ISF format, magnitude nomenclature is restricted to five characters. The recommended magnitude nomenclature is intended to be consistent with nomenclature that has been used by editorial boards of the Bulletin of the Seismological Society of America, except that the recommended nomenclature does not subscript characters and uses a hyphen in place of parentheses in order to reduce character count. The representation of the magnitude names in italics is for the purpose of distinguishing nomenclature from regular text in the present section of this Information Sheet; we do not consider italics an element of nomenclature. The recommended nomenclature differs from other widely used current nomenclatures. Relationships between nomenclatures are illustrated in Table 3.

In Table 3 **"BSSA editorial style"** is the nomenclature that seems to us most representative of style recommended in recent decades by editors of the Bulletin of the Seismological Society of America**. "NMSOP generic"** and **"NMSOP specific"** are respectively the "generic" and "specific" nomenclature used in the first edition of the IASPEI New Manual of Seismological Observatory Practice (Bormann, 2002a, 2002b). In the specific nomenclature the general magnitude symbol M is followed by the symbol of the seismic phase and then by the symbol of the component (V – vertical; H – horizontal) on which amplitude is measured. Then the first letter(s) in brackets stand(s) for the instrument type on which magnitude is measured: e.g., A = WWSSN-SP, B= WWSSN-LP, D = velocity broadband, WA = Wood Anderson. Further symbols/names stand for specific calibration functions used, e.g., "CF" for California and "Author" for author- or agency specific calibration function. "USGS Search" is the nomenclature used by the USGS/NEIC in its Earthquake Catalog Search (http://neic.usgs.gov/neis/epic/, last accessed March 2012). "USGS EDR" is the nomenclature used by the USGS/NEIC in its on-line machine-readable Earthquake Data Reports (ftp://hazards.cr.usgs.gov/edr/, last accessed March 2012). "ISC" is the nomenclature historically used by the International Seismological Centre. USGS/NEIC and ISC nomenclature has changed as advances in information technology have permitted greater flexibility in nomenclature.

Table 3 A sample of alternative nomenclatures for the magnitude types that are considered in this report. For detailed explanation see text.

This report	BSSA editorial style	NMSOP generic	NMSOP specific	USGS Search	USGS EDR	ISC
ML	M_L	Ml	MH(WA;CF), MV(WA;CF)	ML	ML	M_L
Ms_20	M_S(20)	Ms	MLV(B)	Ms	MSZ	Ms
Ms_BB	M_S(BB)	Ms	MLV(D)	--	--	Ms
mb	m_b	mb	MPV(A)	mb	MB	Mb
mB_BB	m_B(BB)	mB	MPV(D)	--	--	mB
mb_Lg	$m_b(L_g)$	mbLg	MLgV(A;Author)	Lg	LG	MN

In conjunction with the full-fledged implementation of the new IASPEI standards, the WG encourages seismological agencies to work toward harmonizing their nomenclatures in order

to minimize misunderstanding on the side of data users and to better guide users' search for standard magnitude data.

3.4 Nomenclature for amplitudes, periods, and amplitude-measurement times

The ISF (IASPEI Seismic Format) data-exchange format that was discussed in the previous section allows for data lines (the ARRIVAL data type) to convey station-specific magnitude data. The amplitude, period, and amplitude-measurement time that is associated with a single magnitude measurement is transmitted on a single line, along with the calculated station-magnitude value. A "phase name" (see **Table 4**) must generally be associated with the data.

Table 4 ISF "phase names" to be used for transmittal of amplitudes, periods, and amplitude-measurement times for the standard magnitude types considered in this paper. "I" stands for "International" or "IASPEI", "A" for displacement amplitude, and "V" for velocity amplitude.

Magnitude type	Phase Name
ML	IAML
Ms_20	IAMs_20
Ms_BB	IVMs_BB
mb	IAmb
mB_BB	IVmB_BB
mb_Lg	IAmb_Lg

3.5 Agency-specific circumstances that may lead to modification of standard procedures

The IASPEI Standard Procedures are proposed for implementation by seismological agencies in general. Adoption of the Standard Procedures by an agency will make that agency's magnitudes more useful to global seismological research and will enable the agency to directly compare its own results with IASPEI standard magnitudes produced by other agencies. The *Magnitude WG* recognizes, however, that agency-specific circumstances may make it desirable for individual agencies to use procedures that differ from the Standard Procedures. In this case, agency documentation and agency-produced bulletins should contain sufficient information to allow a user to understand how the agency's magnitudes can be related to magnitudes produced by the Standard Procedures.

For situations in which data demand modifications to the attenuation equations that are specified in the Standard Procedures, we recommend the practice that has been followed in the historic development of magnitude scales: the current standard equations are to be used as baselines for defining otherwise arbitrary constants in the improved equations. An agency

magnitude-type that is commonly, or in certain magnitude ranges, biased by more than 0.1 magnitude unit with respect to the magnitude produced by an IASPEI Standard Procedure should be identified by nomenclature that is distinct from the IASPEI magnitude nomenclature.

Note: The preceding material of this section (3) was reproduced with minor modification from IASPEI (2013). A following subsection in IASPEI (2011 and 2013), entitled **"DOCUMENT-ATION OF STATION/AGENCY MAGNITUDE PROCEDURES,"** has been attached in NMSOP-2 as Annex 2 to IS 3.4 "Guidelines for using the IASPEI standard magnitude reference data set". This permits seismic stations/agencies to respond to this questionnaire in conjunction with the invitation to analyze the standard magnitude reference data set. In fact, this is the first practical step to educate and train station/agency personnel in the application of the IASPEI standard procedures in comparison with their traditional practices of magnitude determination.

4 Relation of IASPEI standard procedures to original magnitude definition and to procedures for measuring magnitudes at different agencies

As summarized in section 2, the IASPEI recommended measurement standards should, as far as possible, produce magnitudes that are consistent with magnitudes of the same type that have been measured for decades from analog seismograms according to original definitions. This aims at assuring continuity of magnitude estimates published in older and younger earthquake catalogs. We outline below to what extent this has been achieved or, if not, what are the reasons and advantages for deviations.

4.1 ML

The local magnitude scale was developed by Richter (1935) for earthquakes in Southern California. The tabulated calibration values according to Richter (1958) are presented in DS 3.1. The more recent Hutton and Boore (1987) formula for Southern California, on which the standard ML(IASPEI) formula (1) is based, agrees well for hypocentral distances R between 50 km < R < 200 km with the Richter calibration values, but produces higher values (up to 0.6 m.u.) for nearby stations (R < 50 km;) and lower (up to 0.24 m.u.) values for more distant stations up to 600 km (see also Fig. 3.30 in Chapter 3). The large effect at close distances is due to the fact that (according to Hutton and Boore) Richter assumed a geometric spreading with $1/r^2$ whereas the observed spreading is $\approx 1/r$.

However, ML(IASPEI) differs from the Hutton and Boore (1987) ML by accounting for the difference in static magnification assumed by the manufacturer of the WA instruments (2800) and the one empirically determined bv Uhrhammer and Collins (1990), which is about 2080. If ML(H-B) is measured on an original WA record then this difference does not matter. However, when compared with ML(H-B) on a WA simulation record one would expect ML(IASPEI) to be larger than ML(H-B) by log(2800/2080) = 0.13 m.u. = constant. Both effects together (i.e., the use of the Hutton and Boore calibration function and the correction for a constant difference in static magnifications) would produce in the epicentral distance range 0 km < D ≤ 600 km differences between ML(Richter 1935 synthesized) and ML(IASPEI) as depicted in Figure 2.

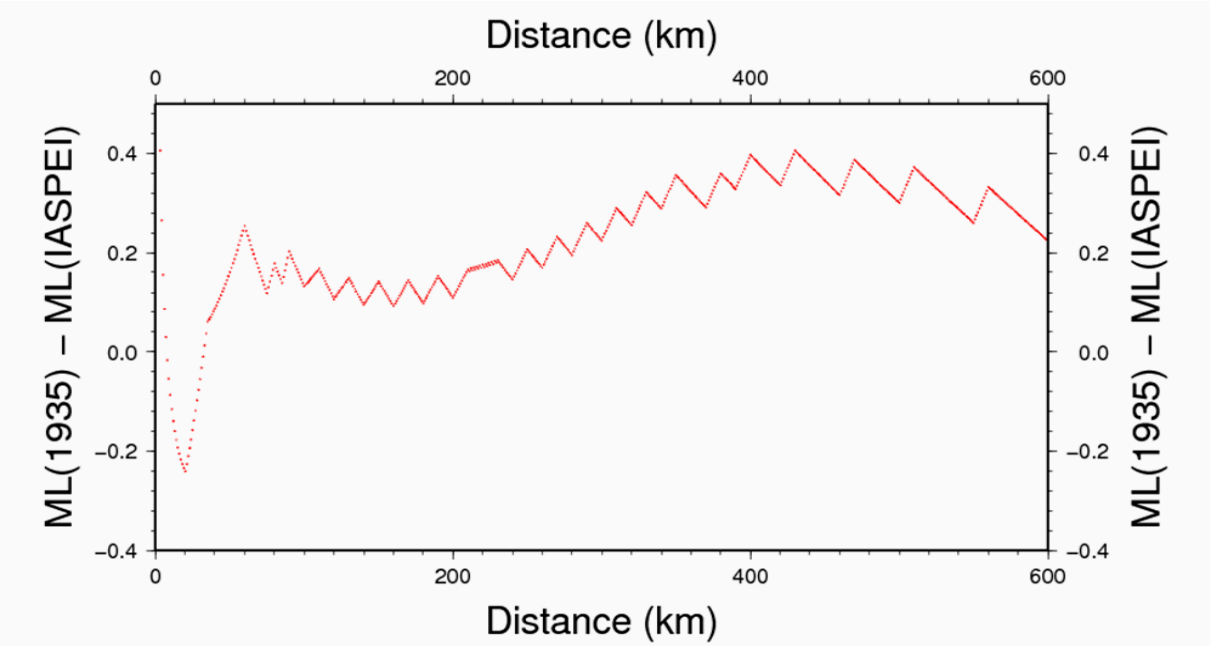

Figure 2 Difference between ML(1935) and ML(IASPEI) as a function of epicentral distance when using, for ML(1935), the Richter (1958) tabulated calibration values (therefore the saw-tooth-pattern in the above figure) and **simulated** WA records assuming a static magnification of 2800 and, for ML(IASPEI), the calibration formula (1) with amplitudes measured on simulated WA records assuming a constant, empirically determined average static magnification of 2080 by Uhrhammer and Collins (1990). This accounts for a constant difference between these two magnitude values of log(2800/2080) = 0.13 m.u. (courtesy of K. Stammler, Federal Institute for Geosciences and Natural Resources, BGR, 2012).

However, as pointed out already by Kim (1998), the difference between the old and the empirically determined WA response **is not constant**, **but frequency-dependent and on average for frequencies at which ML is typically measured, about 0.1 m.u., i.e., 0.03 m.u. less than assumed in Figure 2**. According to D. Bindi (2011, personal communication) the difference varies from 0.065 m.u. at the WA eigenperiod of 0.8 s to 0.13 m.u. at about 8 times longer and shorter periods, respectively, because the damping parameter of the recalibrated WA is not 0.8 (as originally assumed) but 0.7 (see Table 1). For more details see *Comment 1.1* in DS 3.1.

4.2 mB (mB_BB)

mB is the original Gutenberg (1945b and c) body-wave magnitude. It was measured on relatively broadband medium-period instruments at periods between 2 s and 20 s (mostly between 5 s and 10 s) (see Abe and Kanamori 1980; Abe 1981 and 1984). The IASPEI recommendation to measure the maximum amplitude within the whole P-wave train, including also depth phases of P, follows the practice of Gutenberg. Gutenberg and Richter (1956a) published calibration functions for vertical and horizontal component amplitudes of P and PP waves as well as for horizontal component amplitudes of S waves amplitudes. The IASPEI standard uses only vertical component P-wave readings. For this reason, and to

reflect other modifications discussed in the following paragraphs, the IASPEI standard nomenclature is specified as mB_BB.

Gutenberg measured the vast majority of mB for earthquakes with magnitudes larger than 6.5. With current velocity BB instruments of high dynamic range it is possible to determine mB_BB down to about magnitude 4 (at best) or 5 (see Bormann et al. 2007 and 2009). The current instruments also permit reliable measurements to be made at periods above 20s. The new standards have therefore broadened the period range within which mB_BB may be measured beyond the earlier *de facto* range, to 0.2 s < T < 30 s.

The other change is that Gutenberg measured the (A/T)max on displacement records. The standard, however, recommends to measure Vmax on velocity broadband records instead and use (Vmax/2π) as a proxy for (A/T)max. As a matter of fact, analysts tend to measure on displacement records Amax/T instead of (A/T)max, yet the former often occurs at longer periods with the tendency to underestimate (A/T)max and thus mB, especially for smaller earthquakes. This has been confirmed by comparing traditional measurements of mB and related T at the Chinese Earthquake Network Center (CENC), based on Kirnos-type of displacement broadband records, with mB(BB) and related T measured on velocity broadband records Despite these differences in old and new measurement practice the agreement between mB(CENC) and mB_BB is on average 1:1 for magnitudes above 6 (the Gutenberg magnitude range); around mB_BB = 5, however, the classical mB(CENC) is about 0.2 m.u. lower (see related Figures Chapter 3 or in Bormann et al., 2009).

In summary: Standard mB_BB agrees for values > 6.0 well with Gutenberg´s mB measured on displacement-proportional medium-period instruments. However, mB_BB is applicable in a wider range of periods and magnitudes than was usually used with traditional mB, is measured directly from Vmax, and is thus more closely and with less scatter related to released seismic energy than the traditional mB.

Therefore, routine measurement of broadband mB_BB should become a must in future, at least for earthquakes with magnitudes above 5.5. Although no knowledge of period is required for calculating mB_BB it should be measured and reported, because the period at which Vmax is observed is, on average, closely related to the corner period of the radiated source spectrum, increases with magnitude and decreases with increasing stress-drop and rupture velocity (see Chapter 3). While for smaller earthquakes recorded with low SNR in broadband records the measured periods may be strongly biased by the periods of dominating microseismic noise, Figure 3 reveals for magnitudes above 6 the expected exponential increase of period with magnitude.

4.3 mb

mb was introduced into global observatory practice with the rapid increase in the number of sensitive short-period seismographs associated with the deployment of the World-wide Standard Seismograph Network (WWSSN), with the installation of arrays of short-period seismographs, and with regional deployments of short-period (SP) seismographs. They were mostly of the type of the WWSSN-SP response, of the later follow-up PDE-response used at the USGS/NEIC, the response used at the International Data Center (IDC, former Preliminary IDC = PIDC) of the CTBTO (see Figure 3) or covering the SP frequency range between about 1 Hz and 4 Hz in a similar way with relative bandwidth of only one to two octaves.

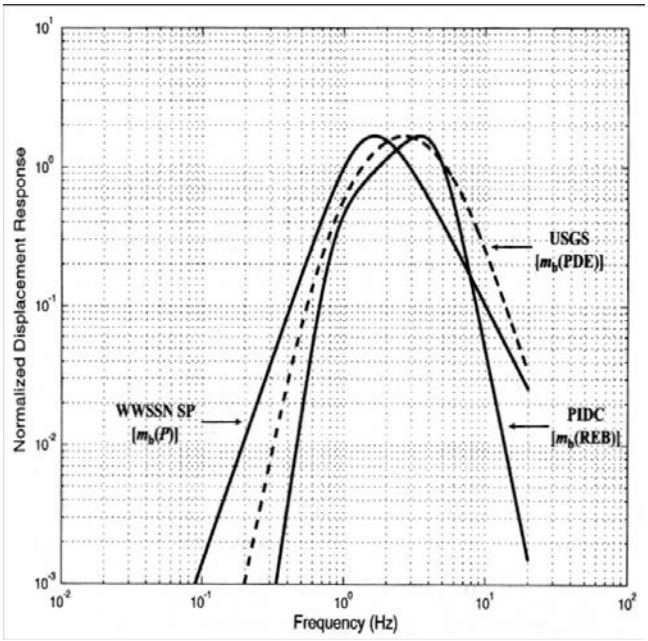

Figure 3 Normalized displacement responses of a typical WWSSN short-period seismograph, of the band-pass filtered record output used by the USGS prior to 2009 for its automatic PDE processing procedure, and the filter response according to the PIDC (now IDC) procedure for short-period data analysis. All responses are normalized to have the same peak gain (modified to same abscissa-ordinate scaling as in Figure 1 from Granville et al., 2005, p. 1813, Fig. 4, © Seismological Society of America).

The high sensitivity of such band-limited short-period seismographs at quiet sites allowed for a dramatic lowering of the size threshold for which teleseismic body-wave magnitudes could be assigned. On the other hand it became clear that for strong earthquakes, mb measurements tend to be systematically less than other types of magnitude , and the effect is dramatic (more than 1 m.u.) for great earthquakes (e.g., Figure 4 in Kanamori, 1983). This effect is sometimes termed "magnitude saturation" (more correctly, a relative insensitivity to increase in the moment of the earthquake). It has two components, a spectral and a rupture-duration related one. Spectral "saturation" begins when the corner frequency of the radiated seismic source spectrum (e.g., Aki, 1967; Geller, 1976; Bormann et al., 2009; and Chapter 3), respectively of the recorded input wave spectrum, is lower than the corner frequency of the seismometer response. With reference to mb and Figure 3 this means that "saturation" is expected to begin earliest for mb(IDC) and latest for mb(WWSSN-SP). Yet mB_BB, measured for periods up to 30 s, saturates accordingly much later than any mb. However, the IDC response allows to measure mb still reliably for smaller events than one can measure on WWSSN-SP records, because of its steeper roll-off and thus improved SNR towards lower frequencies and its peak magnification at 2 times higher frequency.

These comparisons give a feeling for the average influence of different SP seismometer responses on mb magnitude estimates. For the cases investigated they are significant (> 0.1 m.u.) for the PIDC = IDC response. Another case will be discussed in section 5.1.2.

Yet, besides differences in seismograph responses used at different agencies and related differences in spectral "saturation" the application of different measurement time-window after the P-wave first onset may become even the dominating factor on the measured mb values. This is surely the case when the rupture duration of earthquakes and especially the time after the P onset at which the largest spectral amplitudes are released significantly exceed the measurement time-window within which (A/T) is measured. Bormann et al. (2009) derived a simple formula for calculating the average rupture duration T_R in its dependence on the largest event magnitude M: $\mathbf{\log T_R = 0.6M - 2.8}$. For individual earthquakes, however, the rupture duration may be up to about 2-3 times longer or shorter than estimated by this simple formula, due to differences in stress drop and rupture velocity.

In the first years of the WWSSN the United States Coast and Geodetic Survey (USCGS) instructed data analysts to measure Amax in the P-wave train within the first 5 half-cycles. Somewhat later this was extended to within the first 5 s after the P-wave onset. The latter practice is still kept by the IDC of the CTBTO (5.5 s after the first P-onset; see Chapter 17). The reason for this time-window setting was that the WWSSN had as one of its main goals not only the best possible detectability of weak events but also the discrimination between natural earthquakes and underground nuclear explosions. And this discrimination capability was enhanced by measuring within such a short early P-wave time-window, within which explosions surely release their maximum of energy. This, however, is usually not the case for earthquakes with magnitudes larger than 6 for which rupture durations - on average – last for more than 6 s. This, probably, led the IASPEI Commission on Practice to propose in its first report of 1972 to extend the measurement time window for P-wave amplitudes to "15 or 25 s".

Yet at some stations routine practice prior to 1972 was to always measure the maximum amplitude within the whole P-wave train. The first author, for example, introduced this practice at the seismological observatory Moxa (MOX), Germany, in 1965. Figure 4 shows a record example from 1965 (Bormann, 1969) and Tab. 3.1 of Chapter 3 gives a data example from the bulletin 1967 (Bormann and Stelzner, 1972).

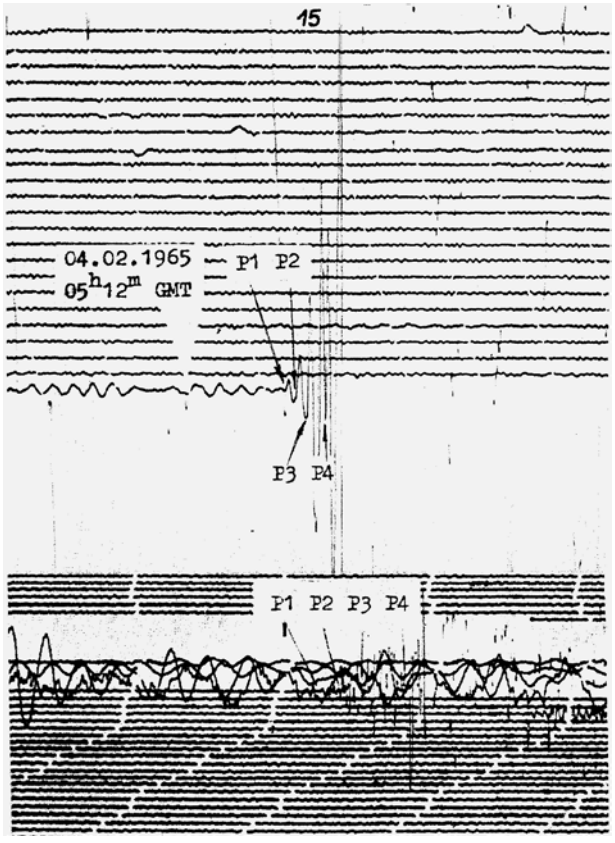

Figure 4 Displacement records of a 1965 Aleutian Islands earthquake at station MOX, Germany. **Below**: Records of type A (SP; 4 octave bandwidth); **Above:** Record of type B (medium period; 8 octave bandwidth). Note the multiple rupture process with P_{max} arriving only 40 s after P1. mb1 = 5.8 and mb4 = 7.0 as compared to mB1 = 6.4 and mB4 = 7.9. When compared with mB1 and mB4,. the spectral underestimation for the more short-period mb1 is -0.6 m.u., for the more long-period mb4 = -0.9 m.u. (Bormann,1969).

The main difference between the traditional Moxa practice and the currently proposed IASPEI mb procedure was that instead of the WWSSN-SP response the Moxa procedure used a more broadband SP type A record, displacement-proportional between 0.8 and 10 Hz. Additionally, in the case of a multiple rupture process, for all major subsequent P onsets, from the initial one up to Pmax, the amplitudes, periods and related magnitudes were measured both in the SP and medium-period (Kirnos SKD) records.

Experience thus collected led Bormann and Khalturin (1975) to state:„…that the extension of **the time interval for the measurement of (A/T)max up to 15 or 25 sec.,** … **is not sufficient** in all practical cases, **especially not for the strongest earthquakes…"** and to recommend in such cases an extension of the measurement to at least 1 min after the first P onset. This recommendation was accepted at the IASPEI meeting in 1976 and included in the Willmore (1979) edition of the Manual of Seismological Observatory Practice. This became also common practice at the USGS/NEIC. Yet, a few extraordinarily large earthquakes confirmed that the rupture duration may last even for several minutes and Pmax arrive even well after 60 s (see record examples in Bormann and Saul, 2008; 2009a). Therefore, Houston and Kanamori (1986) proposed to measure m_b from the maximum amplitude over the whole P waveform recorded on WWSSN-SP records, without setting a fixed time-window limit, as now recommended by the new IASPEI standard.

A consequence of the different practices of mb measurement, both with respect to the frequency responses and measurement time windows used, has been rather different correlation relationships between mb and Ms (see Chapter 3, section "Relationships between magnitude scales") as well as between the mb values of different agencies. Bormann et al. (2007; Figure 2, courtesy of S. Wendt, 2003) showed that the difference between mb(PDE) and mb(PIDC) is on average +0.06 m.u. for mb(PDE) < 4.0, +0.38m.u. for mb(PDE) between 4.0-4.9, +0.48 m.u. for mb(PDE) between 5.0-5.9 and 0.61 for mb(PDE) > 5.9, and that it reached +1.5 m.u. for the great Mw9.3 Sumatra 2004 earthquake with mb(PDE) = 7.2. The IASPEI (2005) recommended mb procedure yielded mb = 7.5 (Bormann et al., 2007) and thus a difference with respect to mb(IDC) of 1.8 m.u.

In contrast, the difference between mb(PDE), measured by the USGS prior to 2009 with the response shown in Figure 3, and the mb(IASPEI_CENC) is much less, where CENC stands for China Earthquake Network Center, which tested extensively the application of the IASPEI standard procedures for magnitude measurement. According to Bormann et al. (2009) the orthogonal regression relationship is

$$\text{mb(PDE)} = 0.90\ \text{mb(IASPEI\_CENC)} + 0.59. \qquad (8)$$

Relationship (8) yields average differences, mb(PDE) – mb(IASPEI_CENC), between +0.14 m.u. and -0.11 m.u. for mb(IASPEI_CENC) between 4.5 and 7.0, but differences may reach 0.5 m.u. for still larger mb values because of the 60 s limit of the old USGS mb measurement time-window.

In summary: since standard mb is measured on simulated records with the same frequency response as early WWSSN records, a significant spectral saturation effect for larger magnitudes remains. However, by measuring Amax in a variable, rupture-duration dependent measurement time-window, the further reduction of mb by using a too short fixed time-window is now avoided. Thus, as shown by Houston and Kanamori (1986) and Bormann et al. (2009), mb values up to about 7.5 can now be measured, giving a more realistic picture of the high-frequency energy release and thus the shaking potential of great earthquakes. For earthquakes with magnitudes below 5-6, however, routine measurement time-windows within the first 5 to 10 s after the P-wave introduce, as a rule, no significant bias. Slight differences of actual WWSSN-SP responses and related simulation filters from the adopted standard may result in average mb differences of about 0.03 m.u. (see, e.g., Figure 11) or, when rounded to the nearest 0.1 m.u., in rounding differences of maximum 0.1 m.u. for about 30% of the events.

4.4 Ms_20

Ms_20 replicates the procedure by which Ms(PDE) has been computed for almost four decades by the USGS/NEIC. Ms_20 is supposed to be closest to the original definition of the surface-wave magnitude by Gutenberg (1945a). This is empirically true yet requires some clarification about significant differences in measurement procedures and applied calibration function. Gutenberg´s Ms formula reads, when A is measured in μm:

$$Ms = \log A + 1.656 \log \Delta + 1.818. \quad (9)$$

It is applicable between $20° \leq \Delta < 130°$ with differences <0.05 m.u. as compared to respective tabulated values in Gutenberg (1945a) (see also DS 3.1 of this Manual). The latter, however, account better than the simple formula for the energy focusing of surface waves towards the antipodes. The differences between Ms values calculated for larger distances according to (9) or by using the tabulated calibration values are 0.07 m.u. at 140°, 0.12 m.u. at 160° and 0.55 m.u. at 180°.

Note, that formula (9) uses only displacement amplitudes A. Gutenberg himself did not note in his notebooks, at which period A had been measured, because he had defined his Ms scale for "periods of about 20 s". As a matter of fact, surface-wave maxima in records of earthquakes with magnitudes > 7 and those with dominatingly oceanic travel paths tend to have periods around 20 s. This was the case for most of the records analyzed at Pasadena in these early years. Moreover, Gutenberg (1945a) and Gutenberg and Richter (1956b) argued that a measurement period of about 20s, in preference to significantly shorter periods, would for earthquakes of focal-depth less than 40 km suppress significant underestimation of Ms that might result from strong depth-dependence of surface-wave excitation at the shorter periods. Yet, comparison with the original bulletins also of other stations used by Gutenberg as data sources for calculating the Gutenberg-Richter M_{GR} magnitudes in "Seismicity of the Earth" (Gutenberg and Richter, 1954) showed that periods as low as 12 s and as high as 23 s were sometimes used, with values outside of the period range 18 s to 22 s not being rare (Abe, 1981; Lienkaemper, 1984).

Further, the Gutenberg formula was derived for scaling horizontal component surface-wave readings, but Gutenberg did not determine the true maximum vector sum of the surface-wave amplitudes in the N-S and E-W component measured at the same time (or within $1/4^{th}$ to $1/2^{th}$ of the measured period, as commonly practiced or assumed). Rather, Gutenberg "vectorially" combined the largest surface-wave amplitudes measured in the two horizontal components although they may arrive at rather different times and belong to different types of surface waves. This may, in the extreme, result in 0.15 m.u. too large magnitude estimates, if both Rayleigh (LR) and Love waves (LQ) have comparably large amplitudes and the backazimuth of wave approach is $0° + n90°$ with n = 0, 1, 2, or 3. An example is shown in Figure 5.

The U.S. Coast and Geodetic Survey, predecessor to the USGS/NEIC, began publishing Ms_20 values in 1968. The U.S. agency formalized the Gutenberg tendency to prefer waves with periods near 20s (the USGS/NEIC uses periods in the 18s – 22s range) but adopted an IASPEI recommendation that the magnitude formula be that of Vaněk et al. (1962)

$$Ms = \log_{10}(A/T)_{max} + 1.66 \log\Delta + 3.3, \ (A \text{ in } \mu m). \quad (10)$$

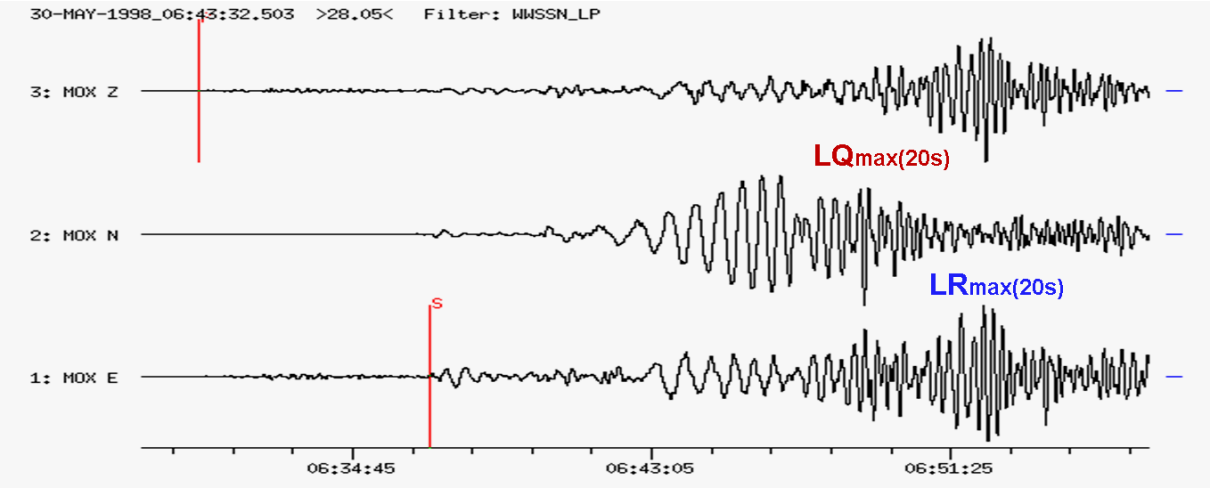

Figure 5 The difference between Ms derived from these records according to the Gutenberg "vectorial" combination $A_{Hmax} = (LR_E^2 + LQ_N^2)^{1/2}$ and the true A_{Hmax} of LR is +0.12 m.u. This is about the largest difference possible (0.15 m.u.) and depends on the BAZ (here 85°).

The U.S. agency procedure also suggested that contributing observatories measure horizontal component surface-wave amplitudes measured at simultaneous arrivals (Lienkaemper, 1984), thus allowing to calculate the true vectorial A_{Hmax}. The latter change, together with some other factors explained by Lienkaemper (1984), makes Ms_20 empirically compatible with the classical Gutenberg-Richter (1954) magnitudes in "Seismicity of the Earth". This is confirmed by Figure 6. For more detailed discussion see Chapter 3.

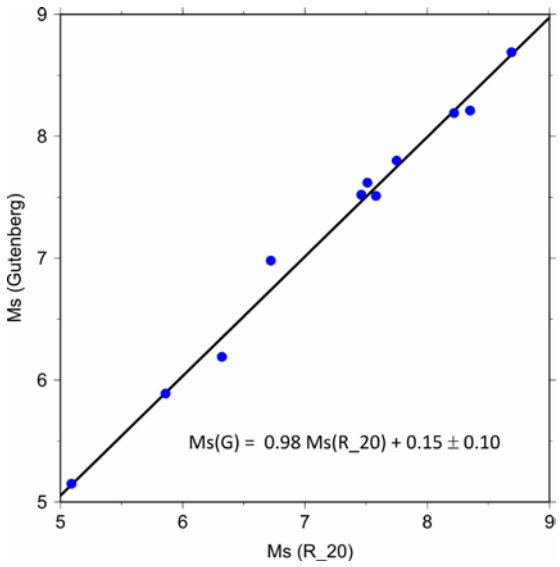

Figure 6 Comparison of Ms(Gutenberg, 1945a) and Ms_20(IASPEI) when vectorially combining for the former the largest N-S and E-W component amplitude readings and for the latter the largest radial (R) surface-wave component amplitude (courtesy of S. Wendt, 2011).

The introduction of stable long-period vertical component (V) seismometers into global seismological practice in the 1960s introduced another change in Ms measurement. According to Hunter (1972) the differences between Ms(V) and Ms(H) are negligible, as confirmed by Bormann and Wylegalla (1975). According to their orthogonal regression relationship

$$MLV = 0.97MLH + 0.19, \quad (11)$$

the two magnitudes differ on average in the range from 4 to 8.5 less than 0.07 m.u.

From May 1975 onwards, the USGS decided to calculate their Ms exclusively from vertical component readings. Since that time, Ms(NEIC) is in fact identical with the IASPEI confirmed standard magnitude Ms_20.

An important feature of the IASPEI Ms_20 formula, equation (3), is that the original formula (10) was derived using data collected over a broader distance range and over a much broader range of periods than the ranges to which the formula is restricted in equation (3). A number of studies, cited in 5.3.3, have suggested that the restriction of equation (3) to periods near 20s produces a distance-dependent bias within the 20° -- 160° distance range to which equation (3) is restricted by the Ms_20 formula. Alternative formulas have been proposed to reduce this bias and to allow extension of the Ms_20 procedure to distances less than 20°.

Ms based on surface waves near 20s are computed by the CTBTO/IDC with an alternative formula (equation 18 of Rezapour and Pearce, 1998) in place of the IASPEI formula, and using data from distances 2° -- 100°, instead of 20° -- 160° (Stevens and McLaughlin, 2001). The Ms_20(IDC) values are published with some delay in the online bulletin of the ISC (International Seismological Centre, http://www.isc.ac.uk/iscbulletin/search/bulletin/, last accessed March 2012). The IDC computes Ms_20(IDC) for nearly an order of magnitude more events than the USGS/NEIC. For events in common, the Ms_20(IDC) values tend to be about 0.1 magnitude units smaller than Ms_20 produced by the USGS/NEIC, although for stations in common the amplitudes computed at the IDC and USGS/NEIC agree to within several hundreths of a magnitude unit on average (Stevens and McLaughlin, 2001).

4.5 Ms_BB

Besides the U.S. preferred practice for calculating Ms_20, there has long existed another tradition of Ms determination in a much wider range of periods between about 2 and 25 s. Even in pre-WWII bulletins of many stations world-wide that were equipped with classical mechanical or electromagnetic medium-period broadband seismographs of Wiechert, Mainka, Bosch-Omori, Galitzin, or similar, one regularly finds readings of surface-wave maxima at periods outside the range of 18-22 s. Since the 1950s, first-rate stations deployed all over the former Soviet Union (FSU) territory and later also in most FSU allied countries of Eastern Europe, as well as those in Mongolia, China, and Cuba have been equipped with displacement proportional broadband seismographs of type Kirnos. The earlier version (SK) had a passband between about 0.1 to 10 s, the later version (SKD) between 0.1 and 20 s (see Figure 10). Using records of these instruments, already Solov´ev (1955) presented empirical evidence that the ratio (A/T) is a stable quantitative characteristic of surface wave maxima, independent of period in a wide range from local to teleseismic distances.

Ms_BB is calibrated with formula (4), only slightly modified from the original formula (10), for inserting directly measured velocity amplitudes in nm/s. The original formula (10) was published by a team of Czech and Russian authors (Vaněk et al., 1962; Karnik et al., 1962) and accepted by IASPEI in 1967 as the standard formula for Ms calculations.

Although formula (10) was originally proposed for the distance range 2° to 160° subsequent work indicates that it is more appropriate to use for distances larger than 140° the tabulated values published by Kondorskaya et al. (1981), which are reproduced in Table 4 of DS 3.1 in this Manual. The reason is the same as the reason that Lienkaemper (1984) used at distances >125° instead of Gutenberg´s (1945a) formula (9) the tabulated calibration values published in Richter (1958) (see Table 3 in DS 3.1), because they better account for the energy focusing effect towards the antipodes.

The Czech and Russian team that developed equation (10) (Vaněk et al., 1962; Karnik et al., 1962) measured the surface-wave maxima in a wide period range between some 2s and 25 s. In Chapter 3 it is shown that Vmax recorded in modern very broadband records may occur, although rarely, at periods well beyond 25 s, up to about 60 s. Accordingly the period range for Ms_BB measurements has been extended now so that it is 3 s < T < 60 s. The Czech and Russian team showed that the prevailing periods depend on distance (Vaněk et al., 1962). Their related Table (see Table 6 in DS 3.1) has been reproduced in the Wilmore (1979) Manual of Seismological Observatory Practice. The Wilmore (1979) Manual also includes the recommendation: "When the period differs **significantly** from the values in Table 3.2.2.1, it may be advisable not to use the data for magnitude determination." The issue of use of the Ms_BB formula beyond the distance-dependent period ranges indicated in Table 6 of DS 3.1 still deserves special study.

The IASPEI proposed procedure for Ms_BB determination has been extensively tested at the CENC, where it was applied to some 10,000 station readings of globally distributed earthquakes recorded by the broadband China National Seismic Network (CNSN) in the distance range between 2° and 100° (Bormann et al., 2009). Despite the large scatter of station-site period readings the general trend and range of periods published by Vaněk et al. (1962) has been confirmed down to local-regional distances and periods as short as 2 to 5 s. Additionally a trend of period increase with magnitude was evident (see also related Figures and discussions in Chapter 3). It is notable that the variance of Ms_BB resulting from this test was somewhat smaller than the variance of Ms_20 (Table 5).

Table 5 Average standard deviations of station magnitude estimates from average network event magnitudes for different scales. Data were taken from Bormann et al. (2007 and 2009). GRSN = German Regional Seismic Network, data by courtesy of S. Wendt; CNSN = China National Seismic Network. Note that CNSN SD values for Ms_20 and Ms_BB relate to readings of equivalent Chinese magnitude standards of Ms7 and Ms, respectively.

Magnitude	Average SD (GRSN)	Average SD (CNSN)
mb	0.21	0.23
mB_BB	0.15	0.21
Ms_20	0.12	0.26
Ms_BB	0.10	0.23

Although Ms_BB and Ms_20 agree well whenever T at Vmax, respectively Amax, is close to 20 s, differences may reach 0.5+ m.u. when T differs (depending on magnitude, travel-path and distance) significantly from 18-22 s (Figure 7).

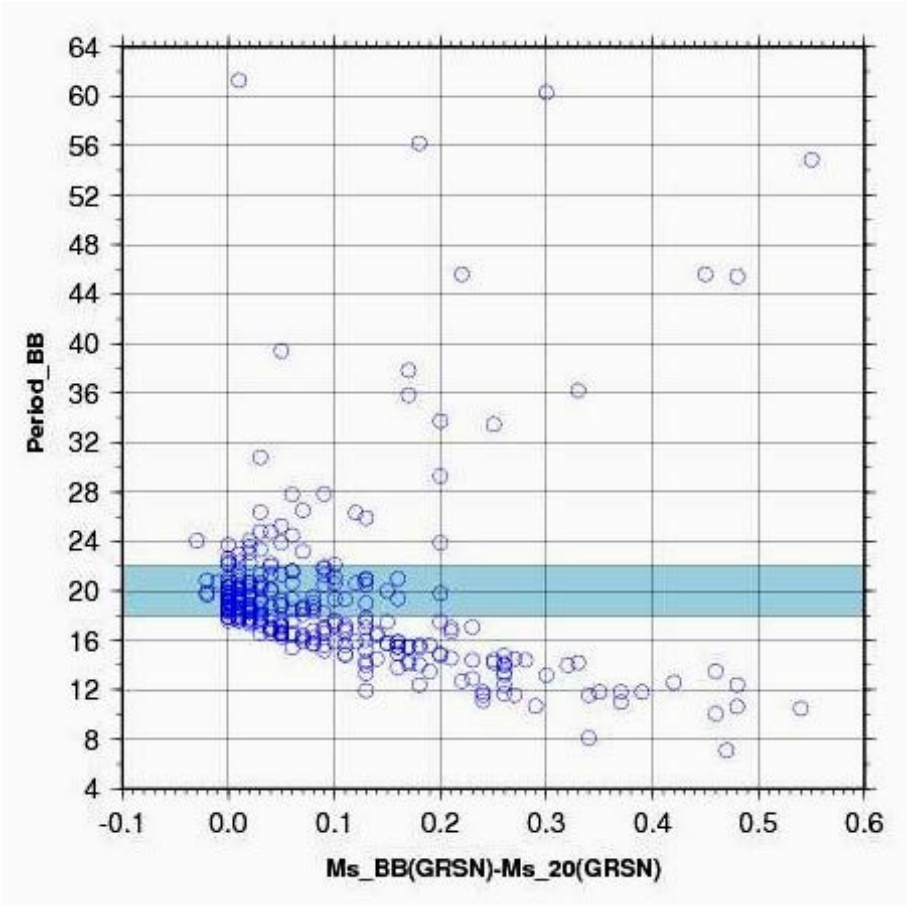

Figure 7 Difference between Ms_BB and Ms_20 in relation to the period at which Vmax was measured on the velocity broadband records. Data are based on GRSN station record readings (courtesy of S. Wendt, 2008).

In the study of Bormann et al. (2009) most of the Vmax values of Rayleigh surface waves were observed outside the period range 18-22s. This holds for 79% of the analyzed CNSN records and for 62% of the analyzed GRSN records (see Figure 7), although the latter include many more oceanic travel paths and rarely any record at epicenter distances below 13°, which are much more frequent in Chinese network records and typical for rather short-period Rayleigh-wave maxima on continents.

Since the two magnitudes are calculated with the same numerical attenuation relation, but surface-wave amplitudes from which Ms_BB can be calculated are commonly larger at periods less than 18 s, the difference Ms_BB – Ms_20 for earthquakes of Ms_BB < 6.5 tends to be 0.1 to 0.2 magnitude units, increasing with decreasing magnitude. But Ms_20 and Ms_BB agree on average rather well for magnitudes above 6.5 (Figure 8). Similarly, both magnitudes agree on average rather well with Mw for magnitudes between 6.5 and 8+ , but for Mw < 6.5 the discrepancy between Ms_20 and Mw is about twice as large as that between Ms_BB and Mw. The magnitude "bias" between Ms_20 and Mw had already been predicted by Kanamori and Anderson (1975) on the basis of theoretical dimension analysis and was empirically confirmed by Ekström and Dziewonski (1988). Recent data by Bormann et al. (2009) fully agree with the theoretically predicted trends for Ms_20 (Figure 9), but also showed that Ms_BB reduces the Ms_20 "bias" for Mw < 6.5 by half.

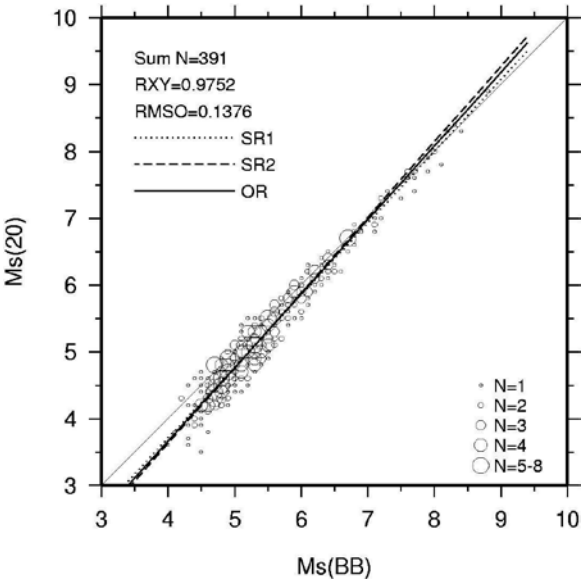

Figure 8 Standard regressions SR1 and SR2 as well as orthogonal regression between Ms_20 and Ms_BB. RXY – correlation coefficient, RMSO – orthogonal root-mean-square error. Cut-out from Figure 11 in Bormann et al. (2009), Bull. Seism. Soc. Am., **99** (3), p. 1881, © Seismological Society of America.

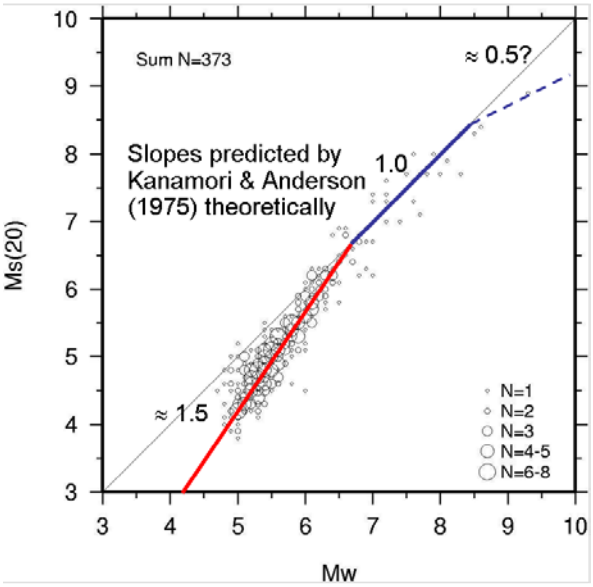

Figure 9 Comparison between CNSN data of standard Ms_20 with Global Centroid Moment Tensor solutions Mw and the theoretically predicted trends by Kanamori and Anderson (1975). Since, according to Figure 14, Ms_BB tends to be larger than Ms_20 for Ms_BB = Mw < 6.5, its bias with respect to Mw is halved in this range.

However, what is or is not considered a bias of a given scale in relation to another is often a matter of perspective or preference given to certain more physically based seismic parameters such as seismic moment or released seismic energy. For example, the reason that Ms_20 scales as 1.5 Mw for small earthquakes is that Ms_20 scales then as $\log M_0$ for these earthquakes. So Ms_20 behaves in a very predictable way with respect to the moment of small earthquakes, and many seismologists find this desirable. Developers of the Ms(Vmax) magnitude (Bonner et al., 2006) specifically emphasize the proportionality of Ms(Vmax) to $\log M_0$ as evidence that Ms(Vmax) is a valuable magnitude. Future comparison of Ms_BB and Ms(Vmax) data, which are now routinely calculated at the USGS/NEIC, will better reveal the benefits or drawbacks, compatibility or complementarity of these two surface-wave magnitudes based on variable period data that are obtained by very different methodologies. In summary: of the two currently adopted IASPEI Ms procedures, Ms_BB agrees best with the original definition and intention of the Ms equation derived by Vaněk et al. (1962). Ms_BB is simply measured on unfiltered velocity broadband records, and several studies have shown that it has lower standard deviations than Ms_20(IASPEI). It is also applicable to many more surface wave records in a wider (down to local) distance range than Ms_20(IASPEI). Moreover, for magnitudes below 6.5 Ms_BB is closer to Mw than Ms_20, irrespective of whether or not this is considered desirable.

4.6 mb_Lg

Nuttli (1973) originally developed *mb_Lg* for eastern North America, and he proposed *mb_Lg* equations for that region that would be reasonable approximations to equations having the form of equations (7) and that are linear in *log(epicentral distance)*. The approximate

equations of Nuttli(1973) implicitly incorporate an eastern North America attenuation function, and the equations are used by many agencies to assign *mb_Lg* to eastern North American earthquakes. The approximate equations of Nuttli (1973) yield *mb_Lg* that are about 0.1 magnitude units smaller than those of the proposed standard procedure, when γ = *.00063 km*$^{-1}$ in equations (7). We propose the procedure of Nuttli (1986) as standard, in preference to the procedure of Nuttli(1973), because the former is transportable to regions with attenuation different than that of eastern North America (Nuttli, 1986; Patton, 2001).

4.7 Mw

The recommended standard formulas for calculating Mw via seismic moment Mo follows directly from the way how it has been systematically derived from the basic assumptions made about the ratio between seismic energy and scalar seismic moment release, average rigidity and stress drop in the source volume and the Gutenberg-Richter relationship between $\log E_S$ and mB on the one hand and mB and Ms on the other hand (see Bormann and Di Giacomo, 2011).

5 Deviations from the recommended measurement standards

The measurement standards specify the frequency response, the period range of measurement, the measurement time-window, the calibration function to be used and how amplitude measurements should be made. Inevitably, different seismological centers will see the desirability to adjust the procedures to address special circumstances. Paradoxically, a chief value in defining standard procedures is to codify a baseline procedure from which the desirability of future improvements to the procedures may be examined. In the following we illustrate examples of the types of *changes in standard procedures that may be acceptable without necessitating that the magnitudes computed with the changed procedure be assigned a different nomenclature.* An alternative procedure may also be preferable to a standard procedure in a particular region if it is more consistent with regional attenuation properties. In this last situation, however, magnitudes computed with the alternative procedure should usually be described with a different nomenclature than magnitudes computed with the standard procedure. For some guidance see IS 3.2.

The first-order criterion to judge whether any alternative procedure is equivalent to a standard procedure is whether or not the alternative procedure yields in a wide magnitude range results that deviate on average less than 0.1 m.u. from those resulting from the strict application of the proposed measurement standards. Alternative proposed measurement parameters will for many purposes be acceptable as substitutes for the standard procedures if it can be confirmed by a representative comparative data set (see IS 3.4), that they do not significantly bias the magnitudes beyond this limit. From a practical standpoint, a changed procedure may be preferable to a standard procedure if, in addition to producing results that are not biased with respect to a standard procedure, it produces results with less scatter than the standard procedure or if it allows unbiased magnitudes to be determined for distance ranges or seismic-noise conditions in which the standard procedure is not appropriate.

The measurement of amplitudes and periods from digital signal by an automatic computer algorithm poses problems that are not addressed by the IASPEI standard procedures. Automatic pickers may require modification of the procedures in order to minimize picking of amplitudes in noisy or prior-shock-contaminated seismograms that would be rejected as

unsuitable by a seismologist who is making measurements with interactive processing software. In cases when a standard procedure is modified to suppress measurements made from noise, the suitability of the modification should be tested with respect to magnitudes that are measured interactively.

5.1 Variations in filter parameters acceptable for determining standard ML, mb, and Ms_20

Figure 10 depicts the responses of seismographs represented in Figure 1 along with responses of several additional seismographs from which magnitude measurements have commonly been made. Unlike Figure 1, where gains are normalized to unity, the relative values of gains in Figure 10 are the ones implemented in the data acquisition and processing system at the Central Seismological Observatory SZGRF of the BGR in Germany (http://www.szgrf.bgr.de/; last accessed 11 March 2012) and the Seismic Handler Motif (SHM) software. We will in the following discuss their suitability for determining standard magnitudes.

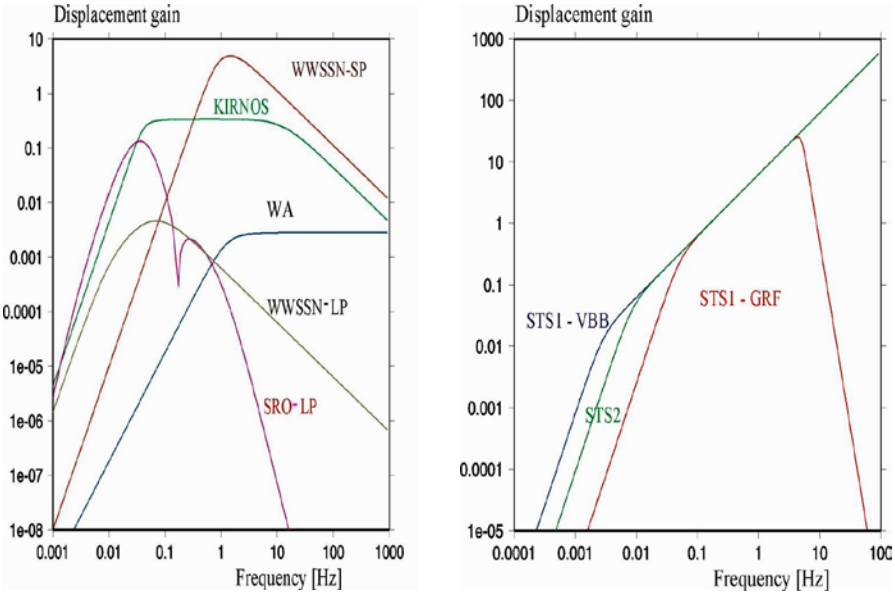

Figure 10 Left: Relative displacement gain of simulation filter responses implemented in the Seismic Handler (SHM) software for analyzing records of the Gräfenberg (GRF) array and of stations of the German Regional Seismic Network (GRSN); **right:** Responses of different generations of velocity broadband seismographs STS1(GRF) (old version used at the GRF array), STS1 (VBB) (advanced version as used in the IRIS global network) and STS2. Figure modified from Chapter 11 to same ordinate-abscissa scale.

5.1.1 ML

According to Figures 1 and 10 (left-hand panel) the response of the Wood-Anderson (WA) seismograph decays with decreasing frequency below 0.5 Hz only with the second order. Accordingly, sea or ocean storm microseisms with frequencies between 0.1 Hz < f < 1 Hz are

not very efficiently suppressed and the signal-to-noise ratio in WA records may become very low for small earthquakes. By increasing the corner frequency of the WA high-pass simulation filter, and/or by steepening its roll-off towards lower frequencies, the SNR may be significantly improved and enable the measurement of ML correctly down to very small earthquakes, provided that the corner frequency of the signal spectrum is still well within the plateau of the modified WA response. Uhrhammer et al. (2011) have used this strategy to enhance SNR for purposes of measuring ML in California.

5.1.2 mb

In section 4.3 we have already extensively discussed the effect of different short-period responses, presented in Figure 3, on mb estimates. With reference to the average seismic source spectrum presented in Figure 1 of Bormann et al. (2009) (see also Chapter 3) we concluded that for magnitudes between about 3.5 and 5.5, the corner frequency of the radiated source spectra and thus the maximum of radiated seismic energy is expected to vary on average between some 0.5 and 4 Hz. When both the relative bandwidth as well as the response peak frequencies within this range differ significantly from the WWSSN-SP standard response then this will result in mb estimates that may differ more than 0.1 m.u. from the IASPEI standard mb as it is the case for mb(IDC). However, the PIDC response (see Figure 3) allows to measure mb still reliably for smaller events than one can measure on WWSSN-SP records, because of its steeper roll-off and thus improved SNR towards lower frequencies and its peak magnification at 2 times higher frequency. Thus it may be an acceptable substitute for the IASPEI standard WWSSN-SP response for mb < 4. A rigorous comparative test is not yet available but would be worthwhile to undertake.

However, also transfer functions for classical WWSSN short-period seismograph differed somewhat for different magnification settings. In addition, different WWSSN-SP simulation filters may have been implemented in different analysis software. For example, the Seismic Handler Motif (SHM) software, developed by Klaus Stammler, BGR Hannover, assumes beyond the response peak only a first-order decay of gain with higher frequencies (see left panel of Figure 10 and poles and zeros in Tab. 11.3 of Chapter 11), in contrast to the decay with second order for frequencies f >3 Hz of the IASPEI adopted WWSSN-SP standard response (Figure 1 and Table 1 in this IS). This effectively means a slight reduction of the relative bandwidth RBW and thus of the measured amplitudes (see Chapter 4). In conjunction with the upgrading of the SHM software to accommodate the new IASPEI standard responses Klaus Stammler filtered about 15,000 P waveforms both with the old SHM and the new IASPEI WWSSN-SP response. He found that mb(IASPEI) would on average be 0.033 m.u. smaller than mb measured on old SHM WWSSN-SP simulated records (with a standard deviation of ±0.06 m.u.) (see Figure 11). Thus, filter-wise the older mb data reported by the BGR to international data centers would still be within the tolerance limit of 0.1 m.u. and thus be acceptable as standard mb values, provided that the variable measurement-time window and peak-to-trough/2 rules have been applied as well. The latter is generally the case in the interactive SHM mode.

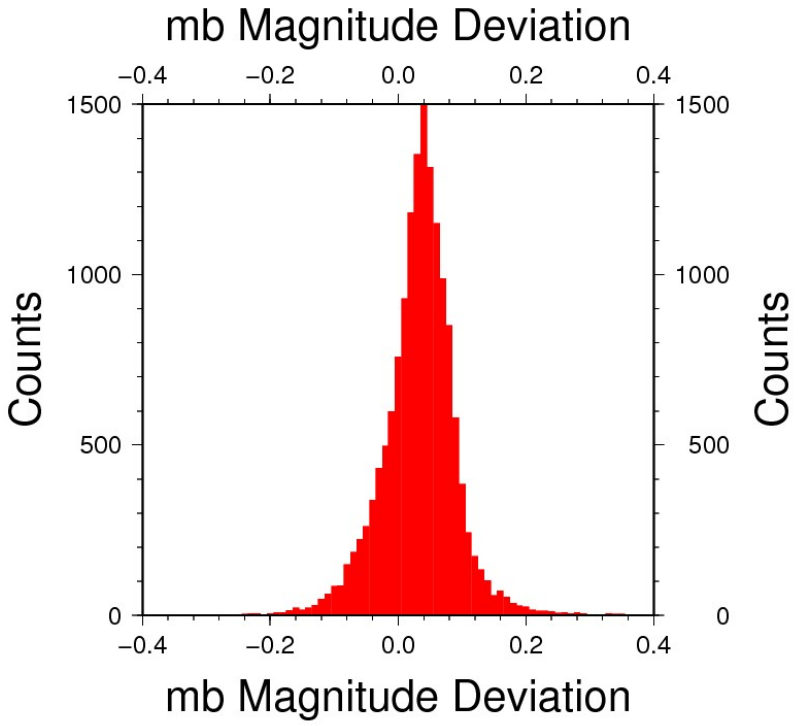

Figure 11 Difference between mb values calculated with amplitudes and periods measured on simulated WWSSN-SP records filtered with slightly different responses: mb(BGR) with the WWSSN-SP response in the left panel of Figure 10 and the poles and zeros in Table 11.3 ?? of Chapter 11 and mb(IASPEI) with the respective response curve and parameters in Figure 1 and Table 1 of this IS 3.3.

5.1.3 Ms_20

According to the standard procedure Ms_20 should be measured on records with the WWSSN-LP response. Yet the instrument's gain decays with increasing frequency only by first order. Therefore, ocean microseisms with periods between approximately 4 to 8 s may result in very low SNR for measurement of surface-waves with periods around 20 s from weak earthquakes. This limits the lower magnitude threshold down to which the mb-Ms_20 criterion for discriminating between natural earthquakes and underground nuclear explosions can be applied (see Fig. 11.22 ??? in Chapter 11 of this Manual). Therefore, a former global U.S. network of Seismic Research Observatories (SRO), operating between 1974 and 1993, used a modified SRO-LP response with much steeper flanks and an additional 6 s microseism notch-filter. This resulted in a rather narrow high-gain 20 s band-pass (see left-hand panel of Figure 10). The difference in shape as well as in the poles and zeros with respect to the WWSSN-LP response is striking (see Table 11.3 ??? in Chapter 11 of this Manual). When compared with WWSSN-LP and velocity broadband records, SRO-LP records look rather smooth and less noisy (Figure 12).

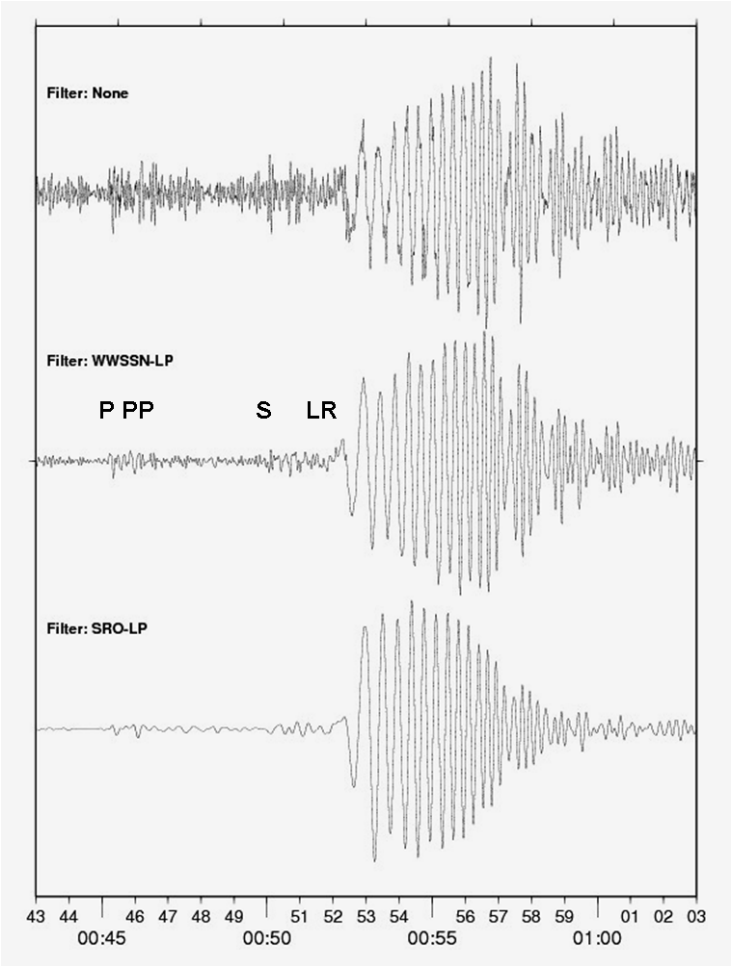

Figure 12 Comparison of an unfiltered STS2 velocity broadband record of an earthquake in the North Atlantic Ocean at station CLL (D = 26.8°, mb = 5.7 (GSR) with the respective WWSSN-LP and SRO-LP filtered records (courtesy of S. Wendt, 2012).

One might expect from so different responses and record appearance significant differences in long-period magnitude estimates. This, however, is not the case for the band-limited Ms_20. Its measurement periods between 18 and 22 s are comparably well covered by the peak-response ranges of both WWSSN-LP and SRO-LP. Therefore, the average relationship between Ms_20 measured on WWSSN-LP and SRO-LP records is indeed 1:1 over the large range of 4 magnitude units with a standard deviation of only 0.03 m.u. (Figure 14), although the respective surface-wave record trains might look quite different (Figure 13a). The data scatter in Figure 14 would only increase somewhat, if WWSSN-LP records with rather low SNR and thus significant amplitude reading errors would be included into the statistics as well. But for surface-wave trains with SNR ≤ 1 in unfiltered velocity and/or WWSSN-LP records it might be possible to determine a reasonably good Ms estimate only from SRO-LP records (Figure 13b).

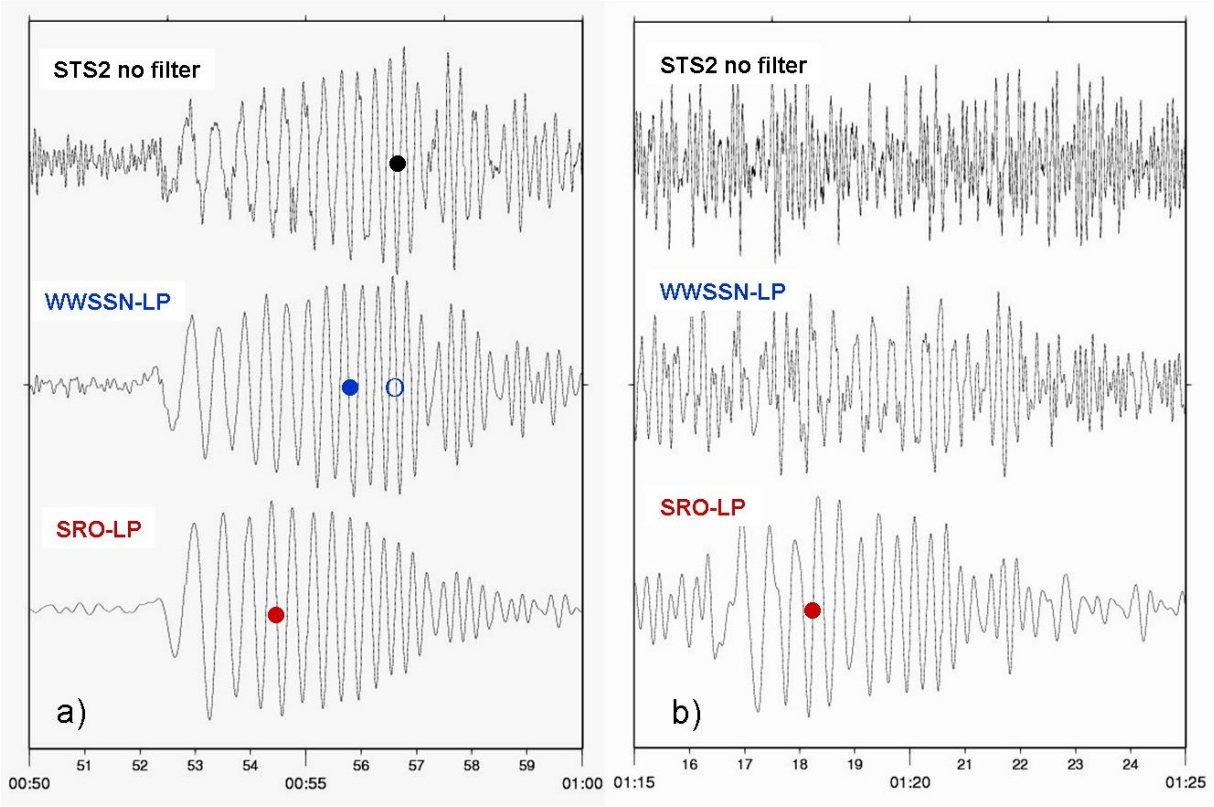

Fig. 13 Unfiltered velocity-proportional STS2 broadband records and related WWSSN-LP and SRO-LP filtered records of the surface-wave train of two earthquakes in the North Atlantic Ocean recorded at station CLL, Germany:

- **a)** 06 Oct. 2011, OT = 00:39:31.0, epicentral distance D = 26.8°, mb = 5.7, Ms_BB = 5.6, Ms_20 (WWSSN-LP and SRO-LP) = 5.5;
- **b)** 06 Oct. 2011, OT = 01:33:33.2, epicentral distance D = 26.7°,mb = 4.5, Ms_20 (SRO-LP) = 4.5.

The solid dots mark the amplitude measurement times for Ms_BB (black) and Ms_20 (blue and red). The open blue circle marks the maximum trace amplitude on the WWSSN-LP record at T = 15.7 s, which would correspond with Vmax on the unfiltered STS2. (Acknowledgment: the figure has been compiled and complemented based on records that were kindly provided by S. Wendt (2012).

From Fig. 13a) one recognizes that the trace Amax is measured earliest on the SRO-LP record at T = 20.3 s and about 80 s later on the WWSSN-LP record within the Ms_20 period window at T = 18.9 s. But the magnitude values are the same, although both being smaller by 0.1 m.u. than Ms_BB, which is measured at T = 15.9 s, about two minutes later than on the SRO-LP record. One should note, however, that in fact also the maximum amplitude in the WWSSN-LP surface-wave train does not occur within the 18-22 s period window, but rather at T = 15.7 s, i.e., close to the period of 15 s at which the WWSSN-LP response has its largest magnification. And when determining log(A/T)max with T = 15.7 s then one gets the same Ms = 5.6 as directly with Ms_BB. Thus, limiting Ms determination on WWSSN-LP records strictly to the narrow period range of 18-22 s is rather arbitrarily fixed to the 20 s spectral amplitude maximum and not related to the maximum record trace amplitude. Yet the 20 s spectral amplitudes are best recorded by a proper SRO_LP filter centered at 20 s.

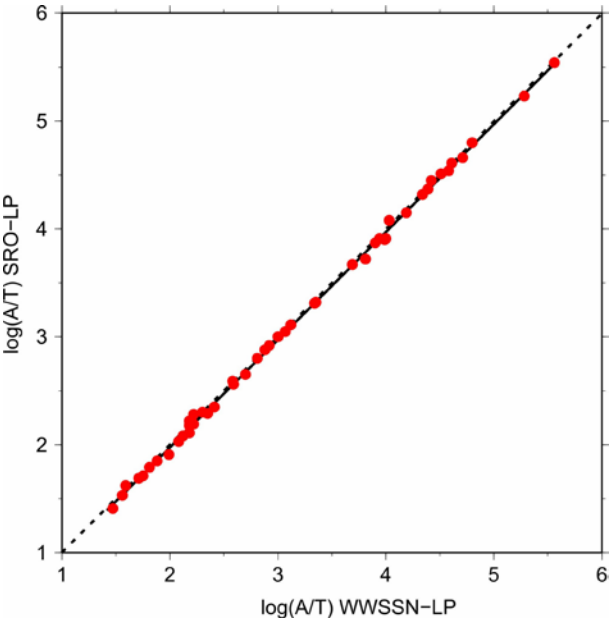

Figure 14 The 1:1 relationship between vertical component maximum Rayleigh wave log(A/T) values measured at periods between 18 and 22 s on SRO-LP and WWSSN-LP records using the IASPEI standard magnitude reference data set (see IS 3.4 of this Manual; courtesy of Siegfried Wendt, 2011).

Figure 14 confirms that Ms_20(SRO-LP) is fully compatible with standard Ms_20. Accordingly, its amplitudes should be reported as IAMs_20. Since SRO-LP records have in any event a better SNR than WWSSN-LP records this would even justify to declare SRO-LP as the best suited response for standard Ms_20 measurements. However, up to now, this filter is less frequently implemented than WWSSN-LP in seismic waveform analysis programs. An exception is the program Seismic Handler (SHM) by Klaus Stammler which can be downloaded from http://seismic-handler.org/portal. Chapter 11 and DS 11.1 to 11.3 present many SRO-LP filtered records in comparison to other standard filtered and unfiltered BB records.

In summary: For Ms_20 determination with the predefined 18 to 22 s period range for measuring A the exact implementation of the WWSSN-LP standard response parameters is not critical, provided that these periods fall within the passband range of any alternative response. Note, however, that neither SRO-LP nor WWSSN-LP narrowband records are suitable to measure correct broadband Ms_BB, which necessitates records with a velocity proportional response which covers the whole range of periods for which this magnitude may be calculated (T = 3 to 60 s), yet at least up to about 40 s. The velocity maximum Vmax of Rayleigh waves occurs only seldom at longer periods. Examples of suitable velocity broadband responses are given in the right-hand panel of Figure 10 with STS2 and STS1-VBB. These frequency ranges are also covered by several more recent broadband systems from the UK, USA and China (see DS 5.1 in this Manual).

5.2 The influence of the measurement time-window on mb and mB estimates

In the above definition of the mb and mB standards it is stated that these body-wave magnitudes should be "…calculated from the maximum trace-amplitude in the **entire P-phase train** (time spanned by P, pP, sP, and possibly PcP and their codas, and ending preferably before PP).

Gutenberg has derived calibration functions for P and PP waves but not for PcP and depth phases. PcP amplitudes are generally smaller than P amplitudes, especially broadband ones

(see, e.g., record examples for event 6 in DS 11.2). So there is no magnitude bias likely from measuring PcP instead of P.

Depth phases were considered by Gutenberg as part of the primary phases with commonly smaller (and then for magnitude estimates irrelevant) amplitudes because of reflection and/or conversion losses as well as extra attenuation along the additional segment of travel. For shallow earthquakes a clear discrimination between superimposed direct and depth phases is difficult anyway and usually beyond the possibilities of routine seismogram analysis. Yet, depth phases may become even larger than their primary phases, as confirmed by both observations (e.g., Figs. 2.62-2.65 in Chapter 2, and Fig. 11.16 ??? in Chapter 11) and synthetic modeling (e.g., Langston and Helmberger, 1975).. The great variability of amplitudes of both P and its depth phases is a source-mechanism dependent function of take-off angle and azimuth and therefore varies with distance and azimuth of the recording station with respect to the source radiation pattern. Procedures such as that of Choy and Boatwright (1995) for calculating released seismic energy E_S and energy magnitude Me assume that the P-wave train consists of direct P plus depth phases and they apply source-mechanism dependent corrections. Since the take-off angles of direct P, pP and sP differ strongly, the inclusion of the depth phases into the mb and mB estimates has an averaging stabilizing effect which reduces possible bias due to strongly variable P-wave radiation when only a limited number of observations with insufficient azimuthal coverage is available.

Also broadband PP amplitudes are usually smaller than those of direct P and especially depleted in higher frequencies because of their longer overall ray path with additional segments through the stronger attenuating upper mantle (see, e.g., record examples of events No. 6 and 7 in DS 11.2). Moreover, onsets of PP are usually well enough separated from P, easy to identify by means of their differential travel-time difference (see differential travel-time curves in Figure 4 of EX 11.2), have their own calibration values (see DS 3.1 in this Manual) and thus are not a biasing factor for P-wave based mb or mB estimates. However, the rupture duration of great earthquakes may be so long that significant amounts of P-wave energy are still arriving at the theoretically expected first arrival time of PP. Should then the measurement time-window **preferably end before PP,** as recommended by the standards**?** Not necessarily, if good reason speaks against it and can be proven by measurement. Figure 15 gives an example for the application of a simple technique, which allows to constrain the appropriate time window in which to search for the maximum P amplitude. It measures the duration *d* of high-frequency radiation, which is mainly generated at the progressing rupture front. Thus *d* is also a rough estimate of the rupture duration T_R but tends to be longer than T_R because of the deliberate inclusion of the depth phases of P and their codas. The technique (for details see (Bormann and Saul, 2008) resembles those of Hara (2007a and b), Lomax et al. (2007), Lomax and Michelini (2009). It computes the envelopes of individual, velocity-proportional P-wave records filtered in a frequency band between 1 and 3 Hz. From the average of all envelopes, aligned by P onset, the time lag is determined at which the amplitude falls below 40% (energy-wise to 16%) of its maximum, thus giving a robust estimate of the approximate duration *d* of the whole P-wave train. It allows to constrain the time window for mb and mB measurements, even in the presence of later phases like PP, which contribute to the high-frequency signal much less than direct P and its depth phases. This is especially useful in automated setups, but simple visual time window selection on the SP-filtered record by an experienced analyst before measuring Amax for mb calculation yields practically the same result.

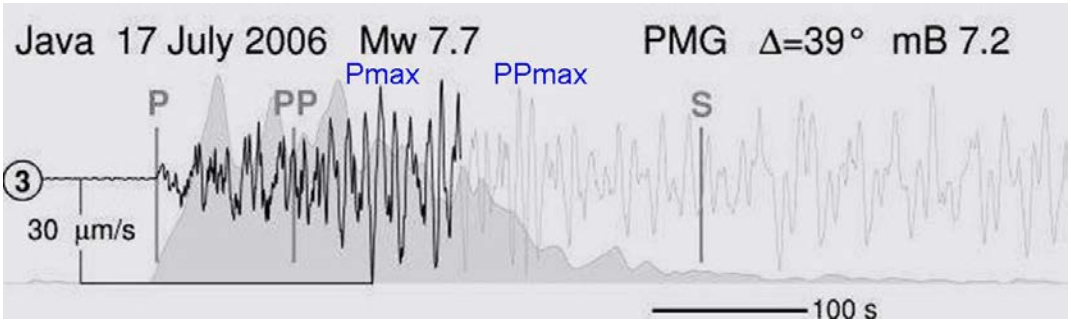

Figure 15 Vertical-component broadband record of the Mw7.7 Java earthquake of 2006 at station PMG. The grey shaded area is the envelope of the positive amplitudes of the velocity-proportional high-frequency (1-3 Hz) filtered P-wave record (plotted at larger scale). Vmax of P is searched within the time-window from the P onset and the time at which the envelope amplitude falls below 40% of the maximum envelope amplitude. This part of the record trace is shown in black. The Pmax, to be measured for mB determination occurs some 140 s after the first P onset, with a period around 10 s, some 50 s later than the theoretically calculated first onset of PP. In contrast, according to the SP envelope, Pmax in the SP record, to be measured for mb, appears already 40 s after the P onset. (Amended cut-out from Figure 3 in Bormann and Saul (2008), Seism. Res. Lett., **79**(5), p. 700, © Seismological Society of America.)

Kanamori (2006), investigating the seismic energy release of the great Mw9.3 2004 Sumatra earthquake, also extended the integration window over the whole P-wave train into the PP range with an estimated bias in E_S that would correspond to less than 0.1 m.u. in Me.

5.3 The influence of the calibration function on the magnitude estimates

The *Magnitude WG* had been entrusted solely with proposing unique measurement standards but not with the development or proposal of new calibration functions. For most magnitude types, the *WG* adopted a strategy of identifying classical, already widely used, attenuation functions as the standard function, with expectation that these functions would be improved upon in the future. The WG endorsed the commonly used practice of using the classical attenuation functions as reference base lines for scaling improved global and regionally specific attenuation functions. Some of such alternative functions exist already but in most cases no agreement has so far been reached for their universal acceptance and use. Below we briefly comment on the current and some of the potential alternative future calibration relationships in order to understand their main differences and possible effects in the case of change.

5.3.1 ML calibration function

The new IASPEI ML standard replaces the old Richter calibration function by the expanded Hutton and Boore (1987) relationship, modified for the Uhrhammer and Collins (1990) recalibration of the Wood Anderson seismograph. The difference from the original Richter formula and its tabulated calibration values has been plotted in Figure 2 (with comments), and the benefits of scaling other regional calibration functions to the H-B formula better at shorter distances than 100 km have already been discussed in section 4.1 of this IS (see also Fig. 3.30

in Chapter 3). Yet, ML differs from most of the other magnitudes in that most ML values are already calculated with region-specific formulas, and they are appropriately designated by unique formulas. The most important principle to establish with ML is that the standard amplitudes are measured through the WA filter and that these amplitudes should be reported in bulletins.

5.3.2 mB_BB and mb calibration functions

Both standard magnitudes are still calibrated with the original revised Gutenberg-Richter (1956a) Q-values for vertical component medium-period P waves (QPZ). The original diagrams and tabulated values are given in DS 3.1, the tabulated values resulting from the USGS scan of the QPZ diagram are presented in Table 2 of this IS for the distance range 20° to 100° as a function of hypocenter depth. The original QPZ(Δ, h) values were given for the distance range 5° to 110°. However, the values in the beginning of the Earth´s core shadow zone of P beyond 100° and in the strongly upper mantle affected distance range between 5° and 20° are considered not yet reliable enough for global application. These problems have already been pointed out much earlier by Evernden (1967) and Booth et al. (1974). A detailed discussion of this issue goes far beyond the scope of this IS and still requires many dedicated investigations which will greatly benefit from the global introduction into observatory practice of the proposed measurement standards. Figure 16, presented in an AGU poster by Saul and Bormann (2007), has been derived from global velocity broadband IVmB_BB amplitude measurements. It may just serve as an illustration of what one can expect, namely a much smoother distance dependence of QPZ in general and major revisions, most likely regionally variable, for distances below 20°. That is, why the current global standards do not yet propose to calculate mb and mB_BB at distances below 20°. We encourage, however, to measure and report to international data centers related amplitude values as IAmb and IV_mB_BB also if they have been measured at distances less than 20° in order to collect masses of standardized data from all seismic regions for investigating such regional variations in amplitude-distance relationships.

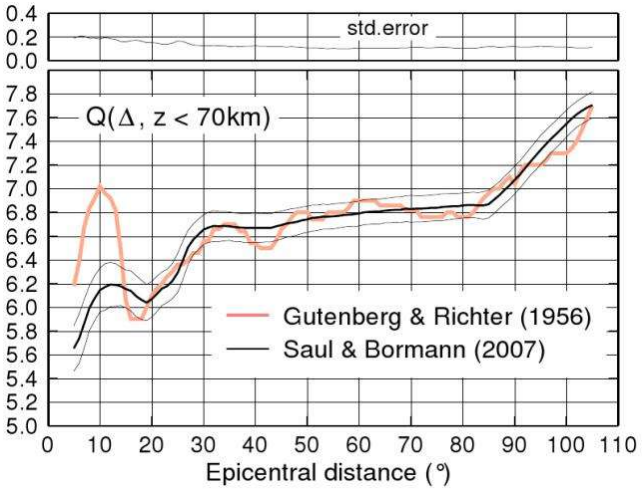

Figure 16 Comparison between the original Gutenberg-Richter (1956a) Q values for vertical component P waves from earthquakes at depth < 70 km with preliminary data based on broadband velocity P-wave amplitude measurements by Saul and Bormann (2007). The Saul and Bormann curve is associated with curves representing +/- the standard error, which is also represented in the chart at the top of the figure.

Veith and Clawson (1972) developed an alternative vertical-component short-period body-wave scale P(Δ, h), which was scaled to the level of the Gutenberg-Richter $Q(\Delta)_{PZ}$ for surface focus. P(Δ, h) is based on WWSSN-SP records from strong explosions. The calibration curves for deeper sources (see Figure 2 of DS 3.1) were calculated using an attenuation model developed by Veith and Clauson 1972). There are large differences between the Gutenberg-Richter and the Veith-Clawson calibration function for deep earthquakes, up to 0.6 m.u. The Veith and Clawson (1972) body-wave scale has been adopted by the CTBTO/IDC, and differences between the Veith and Clawson P(Δ, h) values and the Gutenberg and Richter Q(Δ, h) values are, for intermediate-depth and deep-focus earthquakes, a significant component of the discrepancy between the mb(NEIC) and mb(IDC) discussed in section 1 (Murphy and Barker, 2003).

In general, there is a need to develop improved global and region-specific calibration functions for both mb and mB, or to confirm some of the various calibration functions that have already been proposed. In addition to the previously discussed global calibration functions of Gutenberg and Richter(1956a) and Veith and Clawson(1972), Murphy and Barker (2003) have tabulated proposed global calibration functions from 0° to 180°, and Christokov et al. (1983), Lilwall (1987), and Rezapour (2003) have tabulated proposed global calibration functions for distances beyond 20°. The effect of frequency dependence on the attenuation of P-waves must also be considered. The ability to confidently use mB calculations from the near regional distance range would allow seismologists to exploit still better the superior potential of mB for yielding less saturating magnitude estimates of strong earthquakes in real time for tsunami early warning and emergency assistance purposes. Greater confidence in the short-period magnitudes assigned to deep earthquakes might shed light on the source physics of these earthquakes. The future work will strongly benefit from world-wide adherence to the newly recommended IASPEI measurement standards, because they will significantly reduce data scatter due to non-standard procedures, thus bringing out more clearly biases in currently assumed empirical and theoretical Earth models.

5.3.3 Ms_BB and Ms_20 calibration function

The empirical stability and global representativeness of Ms_BB measurements (see section 4.5) notwithstanding, there are a number of factors that would be expected to produce biased station Ms_BB in some seismotectonic settings. "Biased results", in the sense used here, would typically be Ms_BB values at regional distances that are significantly different than the values at teleseismic distances. Marshall and Basham (1972) summarize a number of such factors. For example, Rayleigh wave amplitudes of periods near 10s, from which Ms_BB might be measured at $\Delta \sim 15°$, are expected to be sensitive to differences in velocity structure and attenuation properties of propagation paths, particularly to the difference between a continental path and an oceanic path, but also to the differences between some types of continental path. Other potential sources of bias are the difference between the source spectrum at long and short periods, which will itself be different for earthquakes of different Mw, and the sensitivity of the Rayleigh-wave spectrum to focal depth and focal-mechanism (Tsai and Aki, 1970). A mass collection of standardized Ms_BB and related amplitude and period values in the years to come will provide a good basis for investigations on possible Ms_BB biases associated with particular seismotectonic environments.

More is already known about the systematic distance-dependent biases of Ms_20 when scaled with the IASPEI recommended standard Ms formula (10) according to Vaněk et al. (1962) (von Seggern,1977; Herak and Herak, 1993; Rezapour and Pearce, 1998). As noted

previously, the IDC of the CTBTO calculates already its Ms with formula (18) of Rezapour and Pearce (1998) (see DS 3.1 and Chapter 17 of this Manual) and is successfully calculating Ms at near-regional and regional distances, in addition to teleseismic distances. A significant component of the distance-dependent bias of formula (10), when used for scaling amplitude measured around 20 s only, is likely to arise from the fact that constants in the adopted Ms_20 attenuation relation, equation (3)/equation (10), were determined with data over a broader range of periods with average T increasing significantly as a function of epicentral distance (see Fig. 8 in Bormann et al.. 2009).

Bormann et al. (2009) showed that the difference of relation (10) to relations given by Herak and Herak (1993) or Rezapour and Pearce (1998) reduces to less than 0.1 m.u. between 50° and 170° when using instead of the calibration term in the IASPEI Ms formula the respective tabulated calibration values in Table 4 of DS 3.1 of this Manual. Using tabulated calibration values instead of an approximated formula was proposed already earlier by Vaněk (1995) with reference to the publication about the homogeneous magnitude system (HMS) studies for Eurasia (Christoskov et al., 1991). Yet between 1° and 130° tabulated and formula-derived Prague-Moscow calibration values agree within 0.02 m.u. The global introduction of a revised Ms_20 specific calibration scale may be reconsidered again after several years of standardized Ms_20 measurements are available.

5.3.4 How amplitude, period and measurement time should be measured

The first sentence in section 3.2, which outlines the IASPEI recommended measurement standards, reads: “The amplitudes used in the magnitude formulas below are to be measured as one-half the maximum peak-to-adjacent-trough (sometimes called “peak-to-peak”) deflection of the seismogram trace.” This recommendation is based on common practice with analog records. Analog records had a very limited dynamic range of about 30-40 db. Most trace amplitudes were measured with low signal-to-noise ratio in the millimeter range, sometimes only 2- to 3-times the thickness of the record trace and with the zero line difficult to fix. By measuring one-half peak-to-trough, relative reading errors could be reduced. This may be the reason why Richter, who initially (Richter, 1935) measured zero-to-peak amplitudes changed later (Gutenberg and Richter, 1956b) to one-half peak-to-trough measurement. This practice also reduces measurement errors when short-period signals are riding over long-period noise or the surface-wave train of a previous earthquake, making it difficult to fix the zero reference line. Moreover, the majority of record signals, especially in narrowband records of the WWSSN-type, and dispersive surface-wave trains anyway, appeared rather symmetric. Empirically, both one-half peak-to-trough and zero-to-peak reading practices yield in many circumstances the same magnitude values to within 0.1 m.u (Rezapour and Rezaei, 2011). Thus it became the dominant practice in older times and continued to be also the easiest and rather unambiguous way of amplitude measurement in modern interactive seismogram analysis programs, because an experienced analyst will always be able to recognize most easily and pick correctly the largest peak and adjacent trough. Accordingly, almost all reading examples presented in the 1979 Willmore Manual of Observatory Practice as well as in the first edition of the NMSOP favor the (P-to-T)/2 approach of amplitude.

However, the problem is more complex. In the first edition of the NMSOP there is also an example given for amplitude measurement on a strongly asymmetric P-wave onset, as they often appear on broadband displacement records. The more broadband a displacement record is, the more asymmetric are the records of body-wave onsets (see the two lowermost record

traces in Fig. 4.13 and Fig. 4.15 of Chapter 4). Many classical medium- to long-period analog seismographs, widely used for measuring mB and Ms in the past, such as those of type Wiechert, Mainka, Galitzin and Kirnos, were more or less broadband displacement recorders. NMSOP then recommends to measure the largest half-swing amplitude from the zero line.

In this context one should be aware that an ideal seismic rupture does not produce an harmonic oscillating ground displacement. Rather, when the rupture can be approximated in a time-displacement diagram by a ramp function in the *near-field* range then this is observed in the *far-field* as a more or less bell-shaped and single-sided displacement pulse (see Fig. 2.4 in Chapter 2), which, if directivity is present, may have asymmetric rise and decay times (e.g., the Brune model displacement pulse in Fig. 4.17 of Chapter 4) Only its time-derivative, i.e., the far-field ground-motion velocity, is a two-sided oscillation with comparable amplitudes. Also narrow-band records in general as well as acceleration and surface-wave records show more symmetric oscillations. The differences in the symmetry of oscillations are very obvious, when comparing in Fig. 4.18 of Chapter 4 the unfiltered velocity broadband and the narrow-band short-period WWSSN-SP and long-period SRO_LP records with the Kirnos and WWSSN-LP displacement records.

Therefore, many algorithms for automatic record analysis prefer zero-to-peak (or trough) measurement, e.g., the current version of SeisComp3 (Hanka et al., 2010) and used for the mB study by Bormann and Saul (2008). Zero-to-peak (trough) measurement can be more easily and unambiguously implemented, even a moving zero-line can most easily be determined by a moving long-term average and de-trending algorithm. Measuring the maximum amplitude between two zero crossings avoids the risk of getting trapped in a secondary minimum or maximum when looking for the largest adjacent trough (or peak).

Clearly, although the *Magnitude WG* has specified a procedure for measuring amplitudes, there is not consensus in the seismological community on the question of optimum procedure for amplitude measurement. Comparative measurements of amplitudes for standard mb, mB_BB, Ms_20 and Ms_BB using both the peak-to-trough/2 and the zero-to-peak (or trough) approach are currently still under way and will be reported soon in a related section of the revised Chapter 3 of this Manual.

The new IASPEI recommended procedure for determining periods differs from the procedure that was commonly used with analog instruments and that is recommended in the 1979 Willmore Manual of Observatory Practice as well as in the first edition of the NMSOP, namely, that period should be read by measuring the time difference between the two neighboring maximum peaks or troughs. The newly recommended procedure -- "…periods are to be measured as twice the time-intervals separating the peak and adjacent-trough from which the amplitudes are measured" -- would have been impracticable using large amplitude analog records with fixed low time resolution and the difficulty to project precisely the time position of the peak down to the level where the time difference to the trough had to be measured. But most modern interactive analysis programs can now perform this easily and give the time of the zero-crossing between the peak and adjacent-trough as the amplitude-phase arrival-times. A modern zero-to-peak amplitude measuring algorithm would use neither the procedure recommended in the earlier manuals nor the current IASPEI recommended procedure: a zero-to-peak algorithm would measure the double time difference between the zero crossings relating to the measured maximum amplitude as period and give the time of the peak position itself as the measurement time. The fully automatic procedure of amplitude and period measurement at the IDC of the CTBTO determines even the period from the three half

periods between which the maximum amplitude has been measured (see Fig. 17.9 in Chapter 17 of this Manual).

For all the IASPEI magnitudes except mb, the value of the magnitude does not actually depend on the measured period. In fact, also mb could be measured directly via Vmax with likely comparable or even better precision than the standard procedure (currently under investigation) after convolving the broadband velocity record directly with the WWSSN-SP response. The cataloging of *T* is, however, important because *T* provides useful supplemental information that can help assess the reliability of a station magnitude measurement and because *T* for some magnitude-types (mB_BB or Ms_BB) contains information about the seismic source that is independent of the information provided by amplitude. Alternative strategies for measuring *T* (e.g., Boore, 1986; Kanamori, 2005) may provide estimates of *T* that are more informative for some purposes (e.g. engineering seismological) than those provided by the IASPEI procedure.

6 Summary

The information sheet outlines both the aim and the rational of the IASPEI (2005 and 2011) recommended measurement procedures for widely used magnitude scales, and emphasizes the need for a unambiguous unique standardized nomenclature for reported and published amplitudes and calculated magnitudes. The new IASPEI magnitude formulas are presented and the essentials of the procedures and parameter ranges outlined, explained in their historical development, critically analyzed with respect to alternative procedures, their significance, range of tolerance and acceptable modifications. The advantages of the (in western countries still uncommon) broadband body and surface-wave magnitudes mB and Ms_BB as compared to the bandlimited magnitudes mb and Ms_20 are highlighted.

Also stressed is the need for overlapping comparative measurements at seismic stations and analysis centers in conjunction with the implementation of the new standard procedures. Previous and the newly recommended standard procedures should be applied to the broadband waveform data from an IASPEI authorized set of reference events and their results be analyzed statistically. As an example of such a comparison the results of Ms_20 determinations on simulated WWSSN-LP and SRO-LP records, respectively, are presented, proving that they yield identical results. Guidelines for carrying out and documenting the results of such a comparative test are presented in IS 3.4.

Finally, future research into improving magnitude calibration functions, especially in the local and regional distance ranges, is strongly encouraged. It is hoped that such investigations will greatly benefit from the expected forthcoming masses of new data based on the agreed IASPEI measurement standards which are hoped to significantly reduce data scatter due to inconsistent or incompatible procedures of magnitude measurements.

Acknowledgments

We are indebted to Members of the IASPEI Working Group on Magnitude Measurements and others who have essentially contributed to the discussions, consensus and results presented above, or made Figures available for this information sheet, in particular Siegfried Wendt, Joachim Saul and Klaus Stammler. We thank George Choy and Morgan Moschetti for

helpful reviews. Any use of trade, firm, or product names is for descriptive purposes only and does not imply endorsement by the U.S. Government.

References

Abe, K. (1981). Magnitudes of large shallow earthquakes from 1904 to 1980. *Phys. Earth Planet. Interiors*, **27**, 72-92.

Abe, K. (1984). Complements to "Magnitudes of large shallow earthquakes from 1904 to 1980", *Phys. Earth Planet. Interiors*, **34**, 17-23.

Abe, K., and Kanamori, H. (1980). Magnitudes of great shallow earthquakes from 1953 to 1977. *Tectonophys.*, **62**, 191-203.

Aki, K. (1967). Scaling law of seismic spectrum. *J. Geophys. Res.*, **72**, 1217-1231.

Boore, D. M. (1986). Short-period *P*- and *S*-wave radiation from large earthquakes: implications for spectral scaling relations. *Bull. Seism. Soc. Am.*, **76**, 43-64.

Booth, D. C., Marshall, P. D., and Young, J. B. (1974). Long and short period P-wave amplitudes from earthquakes in the range 0°-114°. *Geophys. Jour. R. Astr. Soc.*, **39**, 523-537.

Bonner, J. L., Russell, D. R., Harkrider, D. G., Reiter, D. T., and Herrmann R. B. (2006). Development of a time-domain, variable-period surface-wave magnitude measurement procedure for application at regional and teleseismic distances, part II: Application and Ms-mb performance, *Bull. Seism. Soc. Am.* **96**, 2, 678-696, doi: 10.1785/0120050056.

Bormann, P. (1969): Some features of seismic body-wave onsets and their consideration in improving source location (in German). In *Veröff. d. Inst. für Geodynamik Jena, Reihe A, Heft 14*, Akademie-Verlag, Berlin, S. 21-32.

Bormann, P. (2002a). Magnitude of seismic events. Section 3.2. In P. Bormann (Editor), *New Manual of Seismological Observatory Practice (NMSOP*), GeoForschungsZentrum Potsdam, Vol. 1, Chapter 3, 16-49.

Bormann, P. (2002b). DS 3.1, Magnitude calibration functions and complementary data. In P. Bormann (Editor), *New Manual of Seismological Observatory Practice (NMSOP*), GeoForschungsZentrum Potsdam, Vol. 2, 8 pp.

Bormann, P., and Khalturin, V. I. (1975). Relations between different kinds of magnitude determinations and their regional variations. *Proceed. XIVth General Assembly of the European Seismological Commission, Trieste, 16-22 September 1974*. Nationalkomitee Geod. Geophys., AdW der DDR, Berlin, 27-39.

Bormann, P., and Di Giacomo, D. (2011). The moment magnitude M_w and the energy magnitude M_e: common roots and differences. *J. Seismology*, **15**, 411-427; doi: 10.1007/s10950-010-9219-2.

Bormann, P., and Saul, J. (2008). The new IASPEI standard broadband magnitude m_B, *Seismol. Res. Lett.* **79** (5), 699-706.

Bormann, P., and Saul, J. (2009a). A fast, non-saturating magnitude estimator for great earthquakes, *Seism. Res. Lett.* **80** (5), 808-816.

Bormann, P., and Wylegalla, K. (1975). Investigation of the correlation relationships between various kinds of magnitude determination at station Moxa depending on the type of

instrument and on the source area (in German). *Public. Inst. Geophys. Polish Acad. Sci*., **93**, 160-175.

Bormann, P., Liu, R., Ren, X., Gutdeutsch, R., Kaiser, D., Castellaro, S. (2007). Chinese national network magnitudes, their relation to NEIC magnitudes, and recommendations for new IASPEI magnitude standards. *Bull. Seism. Soc. Am.*, **97**, 114-127.

Bormann, P., Liu, R., Xu, Z., Ren, K., Zhang, L., Wendt S. (2009). First application of the new IASPEI teleseismic magnitude standards to data of the China National Seismographic Network, *Bull. Seism. Soc. Am.* **99** (3), 1868-1891; doi: 10.1785/0120080010

Choy, G. L., and Boatwright J. (1995). Global patterns of radiated seismic energy and apparent stress, *J. Geophys. Res.* **100**, 18,205-18,228.

Christoskov, L., Kondorskaya, N. V., and Vaněk J. (1991). Homogeneous magnitude system with unified level for usage in seismological practice, *Studia geoph. Et geod.* **35**, 221-233.

Christoskov, L., Kondorskaya, N. V., and Vanek, J. (1983). Homogeneous magnitude system of the Eurasian continent: S and L waves. *World Data Center A for Solid Earth*, Boulder Report SE-34.

Ekström, G., and Dziewonski, A. M. (1988). Evidence of bias in estimations of earthquake size. *Nature*, **332**, 319-323.

Evernden, J. F. (1967). Magnitude determination at regional and near-regional distances in the United States. *Bull. Seism. Soc. Am.*, **57**, 591-639.

Geller, R.J. (1976). Scaling relations for earthquake source parameters and magnitudes. *Bull. Seism. Soc. Am.*, **66**, 1501-1523.

Granville, J. P., Kim, W.-Y., and Richards, P. G. (2002). An assessment of seismic body-wave magnitudes published by the Prototype International Data Centre. *Seism. Res. Lett*., **73**(6), 893-906.

Granville, J. P., Richards, P. G., Kim, W.-Y., and Sykes, L. R. (2005). Understanding the differences between three teleseismic m_b scales. *Bull. Seism. Soc. Am.*, **95**(5), 1809-1824.

Gutenberg, B. (1945a). Amplitudes of surface waves and magnitudes of shallow earthquakes. *Bull. Seism. Soc. Am.*, **35**, 3-12.

Gutenberg, B. (1945b). Amplitudes of P, PP, and S and magnitude of shallow earthquakes. *Bull. Seism. Soc*. Am., **35**, 57-69.

Gutenberg, B. (1945c). Magnitude determination of deep-focus earthquakes. *Bull. Seism. Soc. Am.*, **35**, 117-130.

Gutenberg, B., and Richter, C. F. (1954). Seismicity of the Earth and associated Phenomena. 2nd edition, Princeton University Press, 310 pp.

Gutenberg, B., and Richter. C. F. (1956a). Magnitude and energy of earthquakes. *Annali di Geofisica*, **9**, 1-15.

Gutenberg, B. and Richter, C.F. (1956b). Earthquake magnitude, intensity, energy, and acceleration (second paper), *Bull. Seism. Soc. Am.*, **46**, p. 105-145.

Hanka, W., Saul, J., Weber, B., Becker. J., Harjadi, P., Fauzi, and GITEWS Seismology Group (2010). Real-time earthquake monitoring for tsunami warning in the Indian Ocean and beyond. Nat. Hazards Earth. Syst. Sci., **10**, 2611-2622; doi: 105194/nhess-10-2611-2010.

Hara, T. (2007a). Measurement of the duration of high-frequency energy radiation and its application to determination of the magnitudes of large shallow earthquakes. *Earth Planets Space* **59**, 227-231.

Hara, T. (2007b). Magnitude determination using duration of high frequency radiation and displacement amplitude: application to tsunami earthquakes. *Earth. Planet Space* **59**, 561-565.

Herak, M., and Herak. D. (1993). Distance dependence of M_S and calibrating function for 20 s Rayleigh waves. *Bull. Seism. Soc. Am.*, **83**, 6, 1881-1892.

Herak, M., Panza, G., and Costa, G. (2001). Theoretical and observed depth corrections for Ms. *Pure Appl. Geophys.*, **158**, 1517-1530.

Houston, H., and Kanamori, H. (1986). Source spectra of great earthquakes: teleseismic constraints on rupture process and strong motion. *Bull. Seism. Soc. Am.*, 76, 19-42.

Hunter, R. N. (1972). Use of LPZ for magnitude. In: *NOAA Technical Report ERL 236-ESL21*, J. Taggart, Editor, U.S. Dept. Commerce, Boulder, Colorado.

Hutton, L. K., and Boore, D. M. (1987). The M_L scale in southern California. *Bull. Seism. Soc. Am.*, **77**, 2074-2094.

IASPEI (2005). Summary of Magnitude Working Group recommendations on standard procedures for determining earthquake magnitudes from digital data. http://www.iaspei.org/commissions/CSOI/summary_of_WG_recommendations_2005.pdf.

IASPEI (2011) Summary of Magnitude Working Group recommendations on standard procedures for determining earthquake magnitudes from digital data. http://www.iaspei.org/commissions/CSOI/Summary_of_WG_recommendations_20130327.pdf

IASPEI (2013). Summary of Magnitude Working Group recommendations on standard procedures for determining earthquake magnitudes from digital data.

http://www.iaspei.org/commissions/CSOI/Summary_WG_recommendations_20130327.pdf

Kanamori, H. (1983). Magnitude scale and quantification of earthquakes, *Tectonophysics* **93**, 185-199.

Kanamori, H. (2005). Real-time seismology and earthquake damage mitigation. *Annu. Rev. Planet. Sci.*, **33**, 195-214.

Kanamori, H. (2006). The radiated energy of the 2004 Sumatra-Andaman earthquake, in: Abercrombie R, McGarr A, Kanamori H (eds): Radiated energy and the physics of earthquake faulting, *AGU Geophys Monogr Ser* **170**, 59-68.

Kanamori, H., and Anderson, D. L. (1975). Theoretical basis of some empirical relations in seismology. *Bull. Seism. Soc. Am.*, **65**, 1073-1095.

Karnik, V., N. V. Kondorskaya, Ju. Riznitchenko, E. F. Savarensky, S. L. Sobolev, N. V. Shebalin, J. Vanek, and A. Zatopek (1962). Standardization of the earthquake magnitude scale. *Studia geoph. et geod.* **6**, 41-48.

Kim, W.-Y. (1998). The M_L scale in Eastern North America. *Bull. Seism. Soc. Am.*, **88**, 4, 935-951.

Kondorskaya, N. V., Z. I. Aranovich, O. N. Solov´eva, and N. V. Shebalin (Eds.) (1981). Instrukciya o poryadke proizvodstva i obrabotki nabludenii na seismicheskich stanciyach ESSN *Inst. Fiziki Zemli Akad. Nauk SSSR*, Moscow, 272 pp.

Langston, Ch. A., and Helmberger, D. V. (1975). A procedure for modeling shallow dislocation sources. *Geophys. J. R. astr. Soc.*, **42**, 117-130.

Lienkaemper, J. J. (1984). Comparison of two surface-wave magnitude scales: M of Gutenberg and Richter (1954) and Ms of “Preliminary Determination of Epicenters”. *Bull. Seism. Soc. Am.*, **74**(6), 2357-2378.

Lillwall, R. C. (1987). Empirical amplitude-distance/depth curves for short-period P waves in the distance range 20° to 180°. *AWRE Report No. O 30/86,* HMSO, London.

Lomax, A., and Michelini, A. (2009). M_{wpd}: A duration-amplitude procedure for rapid determination of earthquake magnitude and tsunamigenic potential from *P* waveforms. *Geophys. J. Int.*, **176**, 200-214; doi: 10.1111/j.1365-246X.2008.03974.x .

Lomax, A., Michelini, A., and Piatanesi A. (2007). An energy-duration procedure for rapid and accurate determination of earthquake magnitude and tsunamigenic potential. *Geophys. J. Int.* **170**, 1195-1209; DOI: 10.1111/j.1365-246X.2007.03469.x.

Marshall, P. D., and Basham, P. W. (1972). Discrimination between earthquakes and underground explosions employing an improved M_S scale. *Geophys. J. R. Astr. Soc.*, **28**, 431-458.

Murphy, J.R., and Barker, B.W. (2003). Revised distance and depth corrections for use in estimation of short-period P-wave magnitudes. *Bull. Seism. Soc. Am.*, **93**, 1746-1764

Nuttli, O.W. (1973). Seismic wave attenuation and magnitude relations for eastern North America. *J. Geophys. Res.*, **78**, 876-885.

Nuttli, O.W. (1986). Yield estimates of Nevada Test Site explosions obtained from seismic Lg waves. *J. Geophys. Res.*, **91**, 2137-2151.

Patton, H. J. (2001). Regional magnitude scaling, transportability, and M_s:m_b discrimination at small magnitudes, *Pure and Applied Geophysics*, **158**, 1951-2015.

Rezapour, M. (2003). Empirical global depth-distance correction terms for mb determination based on seismic moment. *Bull. Seism. Soc. Am.*, **93**, 172-189.

Rezapour, M., and Pearce, R. G. (1998). Bias in surface-wave magnitude M_S due to inadequate distance corrections. *Bull. Seism. Soc. Am.*, **88**, 1, 43-61.

Rezapour, M., and Rezaei, R. (2011). Empirical distance attenuation and the local magnitude scale for northwest Iran, *Bull. Seism. Soc. Am.*, **101**, 3020-3031.

Richter, C. F. (1935). An instrumental earthquake magnitude scale. *Bull. Seism. Soc. Am.*, **25**, 1-32.

Richter, C. F. (1958). Elementary seismology. *W. H. Freeman and Company*, San Francisco and London, viii + 768 pp.

Saul, J., and Bormann, P. (2007). Rapid estimation of earthquake size using the broadband P-wave magnitude mB. *Eos, Transactions, American Geophysical Union, AGU 2007 fall meeting*, **88**, no. 52, Suppl., Abstract S53A-1035.

Soloviev, S. L. (1955). Classification of earthquakes in order of energy (in Russian). *Trudy Geofiz. Inst. AN SSSR*, **30**, 157, 3-31.

Stevens, J.L., and McLaughlin, K.L. (2001). Optimization of Surface Wave Identification and Measurement, *Pure appl. Geophys.*, **158**, 1547-1582.

Tsai, Y.-B., and Aki, K. (1970). Precise focal depth determination from amplitude spectra of surface waves. *J. Geophys. Res.*, **75**, 5729-5743.

Uhrhammer, R. A., and Collins, E. R. (1990). Synthesis of Wood-Anderson seismograms from broadband digital records. *Bull. Seism. Soc. Am.*, **80**, 702-716.

Uhrhammer, R. A., Hellweg, M., Hutton, K., Lombard, P., Walters, A. W., Hauksson, E., and Oppenheimer, D. (2011). California Integrated Seismic Network (CISN) local magnitude determination in California and vicinity. *Bull. Seism. Soc. Am.,* **101**, 2685-2693.

Utsu, T. (2002). Relationships between magnitude scales. in Lee, W.H.K., Kanamori, H., Jennings, P.C., and Kisslinger, C., (eds.). International Handbook of Earthquake and Engineering Seismology, v. 81A, Chapter 44, p. 733 – 746.

Vaněk, J. (1995). Comment on "distance dependence of Ms and calibrating function for 20 second Rayleigh waves, by M. Herak and D. Herak, *Bull. Seism. Soc. Am.*, **85,** 961.

Vaněk, J., Zapotek, A., Karnik, V., Kondorskaya, N.V., Riznichenko, Yu.V., Savarensky, E.F., Solov'yov, S.L., and Shebalin, N.V. (1962). Standardization of magnitude scales. *Izvestiya Akad. SSSR., Ser. Geofiz.*, **2,** 153-158 (108-111 in the English translation).

Veith, K. F., and Clawson, G. E. (1972). Magnitude from short-period P-wave data. *Bull. Seism. Soc. Am.*, **62**, 435-452.

von Seggern, D. (1977). Amplitude-distance relation for 20-second Rayleigh waves. *Bull. Seism. Soc. Am.*, **67**, 405-411.

Willmore, P.L. (1979). Manual of Seismological Observatory Practice. World Data Center A for Solid Earth Geophysics, Report SE-20, September 1979, Boulder, Colorado, 165 pp.